MODELING PRODUCTION OF ACETIC ACID BY OXIDATION OF ETHYLENE WITH ASPEN PLUS

A MASTER'S THESIS

in

Chemical Engineering and Applied Chemistry

Atilim University

by

ABIR ABDELFTAH ALI MAIUF

APRIL 2018

MODELING PRODUCTION OF ACETIC ACID BY OXIDATION OF ETHYLENE WITH ASPEN PLUS

A THESIS SUBMITTED TO

THE GRADUATE SCHOOL OF NATURAL AND APPLIED SCIENCES

OF

ATILIM UNIVERSITY

BY

ABIR ABDELFTAH ALI MAIUF

IN PARTIAL FULFILLMENT OF THE REQUIREMENTS FOR THE DEGREE OF

MASTER OF SCIENCE

IN

CHEMICAL ENGINEERING AND APPLIED CHEMISTRY

AT

THE DEPARTMENT OF CHEMICAL ENGINEERING AND APPLIED CHEMISTRY

APRIL 2018

Approval of the Graduate School of Natural and Applied Sciences, Atılım University.

_____

Prof. Dr. Ali Kara
Director

I certify that thesis satisfies all the requirements as a thesis for the degree of Master of Science.

_____

Prof. Dr. Atilla Cihaner
Head of Department

This is to certify that we have read the thesis "Modelling production of acetic acid by oxidation of ethylene with Aspen Plus" submitted by "Abir Abdelftah Ali Maiuf" and that in our opinion it is fully adequate, in scope and quality, as a thesis for the degree of Master of Science.

_____

Asst. Prof. Dr. Enver Güler
Supervisor

Examining Committee Members

Asst. Prof. Dr. Enver Güler _____

Asst. Prof. Dr. Hakan Kayı _____

Asst. Prof. Dr. Erhan Bat _____

Date: 17.04.2018

I declare guarantee that all data, knowledge and information in this document has been obtained, processed and presented in accordance with academic rules and ethical conduct. Based on these rules and conduct, I have fully cited and referenced all material and results that are not original to this work.

Name, Last name: Abir Abdelftah Ali Maiuf

Signature:

ABSTRACT

MODELING PRODUCTION OF ACETIC ACID BY OXIDATION OF ETHYLENE WITH ASPEN PLUS

Abdelftah Ali Maiuf, Abir
M.Sc., Chemical Engineering and Applied Chemistry
Supervisor: Asst. Prof. Dr. Enver Güler
April 2018, 81 pages

This study investigates the design and optimization model of acetic acid production by oxidation of ethylene using Aspen Plus software. The input to simulation process is the vapor feed stream with CO_2, N_2 as bottom stream and H_2O as top input stream. The research aims to understand and study the production process of acetic acid and study the operational variables and their effects on the production. According to simulation model, the acetic acid has been produced as liquid in bottom stream after six stages inside absorber. Moreover, the flow rate, temperature and pressure have been controlled and analyzed as sensitivity parameters. The basic product is acetic acid produced with mole flow about 0.6 kmol/hr and the mole fraction about 0.004 at 30.3 °C temperature and 10 bar pressure.

Keywords: Acetic acid, simulation, Aspen Plus, sensitivity analysis, modeling.

ÖZ

ETİLEN OKSİDASYONUYLA ASETİK ASİT ÜRETİMİNİN ASPEN PLUS KULLANILARAK MODELLENMESİ

Abdelftah Ali Maiuf, Abir

Yüksek Lisans, Kimya Mühendisliği ve Uygulamalı Kimya

Danışman: Yrd. Doç. Dr. Enver Güler

Nisan 2018, 81 sayfa

Bu çalışmada etilenin oksidasyonu ile asetik asit üretiminin tasarım ve optimizasyon modeli Aspen Plus yazılımı kullanılarak incelenmiştir. Simülasyon işleminde girdi alt akış olarak CO_2, N_2 ile gaz fazı besleme akışı, üst girdi akışı olarak ise H_2O'dur. Araştırma, asetik asit üretim sürecini anlamayı ve incelemeyi ve buna ek olarak operasyonel değişkenleri ve bunların üretim üzerindeki etkilerini incelemeyi amaçlamaktadır. Simülasyon modeline göre, asetik asit absorber içinde altı aşamadan sonra alt akışta sıvı olarak üretilmiştir. Ayrıca akış hızı, sıcaklık ve basınç kontrol edilmiş ve hassasiyet parametreleri olarak analiz edilmiştir. Elde edilen temel ürün, 30.3 °C sıcaklıkta ve 10 bar basınçta mol akışı yaklaşık 0.6 kmol/saat ve mol oranı yaklaşık 0.004 olan asetik asittir.

Anahtar Kelimeler: Asetik asit, simülasyon, Aspen Plus, hassasiyet analizi, modelleme

Dedicated to my husband and family

ACKNOWLEDGEMENTS

I would like to express my sincere gratitude to my thesis supervisor Asst. Prof. Dr. Enver Güler for his kind support, guidance, understanding, encouraging advices, constructive criticism and valuable discussions throughout my thesis.

Then, I would like to express my deepest gratitude to my family whom I owe a great deal, to my father and mother, and like to extend my sincere gratefulness to my friends who have been waiting for my work achievement.

I would also like to thank everyone who has participated in this work and helped me to present it in the best possible manner.

TABLE OF CONTENTS

LIST OF FIGURES

LIST OF TABLES

CHAPTER 1

INTRODUCTION

1.1 OVERVIEW

Acetic acid, is one of most important chemical compound in our life, which is known by the special odor and sour taste. In fact, that sour taste comes from vinegar, which nearly from 4 to 8% are acetic acid. Before recorded history of humans, acetic acid has been producing and utilizing. As same as its taste, the name are comes from the Latin of vinegar, acetum as well. The acetic acid structure has been investigating, and controlled as chemical form (CH_3COOH) in the gas state by infrared spectroscopy and electron diffraction [1-3].

Generally, vinegar is created by dilute solutions of alcohol like wine, by the action of certain bacteria in the oxygen. To finish process bacteria require oxygen while overall chemical change is the reaction of ethanol with oxygen to form acetic acid and water as showing in equation (1-1):

$$CH_3CH_2OH + O_2 \rightarrow CH_3COOH + H_2O \qquad 1.1$$

The acetic acid has several useful effects to human. Mineral deposits are left when the hard water evaporates. Then vinegar is used to remove the residue formed on plumbing fixtures and also that in tea kettles, dissolve in acids. In addition, vinegar inhibits the bacteria growth, so vinegar is utilized as a preservative in foods because it is acidic, like pickled vegetables, and as a mild disinfectant in cleaning.

Although of their importance, the acetic acid (CH_3COOH) is known as one of simplest organic carboxylic acid. Acetic acid as colorless acid features by distinctive sour taste and pungent smell. In industry today, the acetic acid is considering as one of the industry key for a lot of industries that contain chemical, detergent, wood and food industries as well. Utilizing petrochemical feedstock the acetic acid, chemically produced. Classic ways, by approach of fermentative alcohol conversion utilizing especial kind of acetic acid bacteria. In addition, methanol carboxylation is the most common production methods among several chemical techniques, which accounting about 65% of international capacity [2]. Ethylene oxidation comes as second place, which is then followed by alkane oxidation processes. These days, acetic acid is one of the most an important component for the industrial production of various chemicals like cellulose acetate, vinyl acetate polymer, dimethyl terephthalate, acetic acid esters or acetic anhydride and calcium magnesium acetate [2].

In 1960 by BASF, it was the first commercial carbonylation process that includes conversion of methanol into acetic acid. The production of acetic acid in ca. with 90% selectivity, has been done utilizing iodide promoted cobalt catalyst with so high pressure (600 atm) and temperature (2300°C) [4]. The Cativa process, producing the acetic acid

utilizing the iridium catalyst unit, which has been commercialized in 1996 by BP-Amoco [5]. By Wang et al., utilized catalysts to synthesis and production acetic acid by ethylene oxidation [4].

Nowadays, in industry, water and acetic acid separation process is one of the most important operation, as cellulose acetate production or in the terephthalic and isophthalic acids synthesis processes [6]. In addition, most of acetic acid production comes from distillation processes. In other words, it is the separation process that separates several components of a liquid solution, which depends on boiling points of the components. That process is done between liquid phase and vapor phase where all components are present in both phases. By boiling, the vapor phase is generated by liquid phase due to vaporization [7]. In chemical industries, acetic acid is important commodity, in fact per year nearly 9 million tons of world demands. In 1997, acetic acid has the demand about 5.4 million tons/year in the World [8]. Main utilize of acetic acid is manufacture of assorted acetate esters, organic compounds and solvents, fungicide as well as preparation of pharmaceuticals. In addition, acetic acid produce the cellulose acetate, which is significant in made film and plastic wares, synthetic fiber and perfumes. As corrosive organic, acetic acid (CH_3COOH) having a burning taste, sharp odor and pernicious blistering properties.

Nowadays, acetic acid is central to all biological energy pathways, where it can be found in oilfield brines, ocean water and rain. At some concentrations, it is effected in many plant and animal liquids. Fruit and vegetable juices fermentation can be produced about 2–12% acetic acid solutions that named as vinegar.

In chemical technology, absorption can be defined as a process in which atoms or molecules transfer from a gas phase into a liquid phase. In addition, there are differences between absorption and adsorption, where absorption the molecules are taken up by a liquid (absorbent, solvent), while for adsorption the molecules are fixed onto solid surfaces. While distillation process is one of the most popular unit operations. In fact, the mechanism of process established on the different boiling points of the materials to split. It is done by mixing two or more components is brought to the boiling point out of many stages of condensation or evaporation tower [9].

This study investigates the design and optimization model of acetic acid production by oxidation of ethylene by modeling using Aspen Plus software. The input to simulation process is the vapor feed stream with CO_2, N_2 and acetic acid in specific concentrations, pressure and temperature in scrubber. From other side, fresh water comes from the top of scrubber tower as second input. This research designs a RadFrac absorption unit, which will scrub acetic acid from CO_2 containing stream. RadFrac is known as rigorous model for simulating all multistage vapor liquid fractionation operations. In Aspen Plus, it can be used to simulate absorption process. RadFrac has the advantage where it can be simulate modeling columns with two liquid phases and chemical reactions in each liquid phase occurring simultaneously, using different reaction kinetics for each of the two liquid phases. Moreover, it investigates the effect of various process parameters such as pressure, temperature, flow rate and number of theoretical stages. The results of process have been investigated and analyzed, and finally conclusions and recommendations are presented.

1.2 PROBLEM STATEMENT

The vapor feed stream to the scrubber is a mixture of CO_2, N_2 and acetic acid. Therefore, acetic acid is to be recovered. Experimentally, it is hard to know the effect of different process parameters such as pressure, temperature, flow rate and number of theoretical stages as well as the quality of product. Because of these reasons, the simulation study has been done by investigating and analyzing the process results to optimize techniques to choose the best design to gain acetic acid from the process stream. On the other hand, it should be separated from CO_2.

1.3 RESEARCH OBJECTIVES

The main aim of this project is to model the production of acetic acid by oxidation of ethylene with Aspen Plus, and sub-objectives can be listed as:

1. To find out and describe of the amounts of produced acetic acid.
2. Simulate the absorption process using ASPEN PLUS.
3. Find out the effect of various parameters as follows:
    - Pressure,
    - Temperature,
    - Flow rate,
    - Number of theoretical stages.

1.4 WORK SCOPE

The scope of work include the following:

- Literature survey.
- Identifying the process parameters.
- Setting up the process components.
- Finding the upper and lower limitations of various parameters.
- Design and development of ASPEN model.
- Checking adequacy of the models developed.
- Presenting and display the direct effects of different composition, pressure, temperature, flow rate, and number of theoretical stages
- Optimizing the model and how it effects process parameters.
- Investigating and analyzing the process results.

1.5 RESEARCH METHODOLOGY

This research aims a design and optimization approach, which is based on modeling of acetic acid production by oxidation of ethylene with ASPEN PLUS Software. The research contains five chapters. First two chapters were theoretical and from chapter three to five were applied chapters.

First chapter contains the general introduction about modeling acetic acid production method by oxidation of ethylene with ASPEN Plus the scope and importance and research methodology.

Second chapter deals with the basics, history of acetic acid production, and its classification within alternative methods of production. Moreover, it contains the study

and introduction of operational variables such as (pressure, temperature, flow rate and number of theoretical stages).

Third chapter, covers experimental methods with an introduction to ASPEN Plus software. It gives some details about ASPEN modeling, process design and description within process flow diagram. In addition to modeling methodology, that part explains the property method, limitations, inputs and outputs. Sensitivity and effects of operational parameters are shown as well in this chapter.

The fourth chapter named as results and discussion, shows research results including some figures, and process parameters and their effects on production system performance. In addition, discussion of all tables and figures are presented along with some conclusions and presenting proposals.

The fifth chapter deals with the conclusions, recommendations and references. The last chapter deals with the appendix.

CHAPTER 2

LITERATURE REVIEW IN INTRODUCTION

2.1 ACETIC ACID

2.1.1 Acetic acid properties

Acetic acid crystallizes in cool temperatures, it is known as glacial acetic acid in pure form. In fact, it is hazardous to work with, in that form, which is extremely corrosive. Some special requiring precautions for protection in that case. The acetic acid concentration is just 5% in Vinegar.

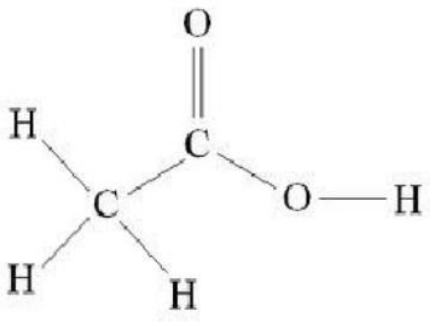

Figure 2.1: Acetic acid chemical form.

Table 2.1: Acetic acid properties

Name	Acetic acid
Molecular Formula	$C_2H_4O_2$
Appearance	clear liquid
Molecular Weight	60.05 g/mole
Density	1.048 kg/m^3
Flash Point	40°C
Boiling Point	117-118°C
Melting Point	16-16.5°C
Storage Temperature	Store at Room temperature
Refractive index	1.3715
Solubility	Miscible with water

Stability

Room temperature acetic acid is stable under normal conditions of handling and storage.

Chemical properties

It is clear colorless liquid, where general description as colorless aqueous solution and smells like vinegar. Lead to corrosive to metals and tissue.

Air and water Reactions

During dilution with water releases some heat.

Reactivity

- With chemical bases, acetic acid reacts exothermic.
- Heat produced by strong oxidizing agents of acetic acid.
- Acetic acid dissolute in water, in ordinary vinegar with 5% solution of acetic acid.

Health Hazard

- Toxic, may cause severe injury or death inhalation if ingested or skin contact.
- Skin and eyes, direct contact with molten substance may cause severe burns, should avoid any skin contact.
- Corrosive or toxic and cause pollution if run off from fire control or dilution water.

Fire Hazard

- Acetic acid burns, but does not ignite readily.
- Hydrogen gas can be produced by contacted acetic acid with metals
- When heated, containers of acetic acid may explode.
- In a molten form, the substance of acetic acid may be transported

2.1.2 Production processes

In chemical industry, acetic acid is produced from fossil fuels as well as by chemicals, which is by three production processes: methanol carbonylation, acetaldehyde oxidation and hydrocarbon oxidation. Moreover, biological routes can be followed as well, by utilizing either an aerobic or an anaerobic route [10]. Primarily, the acetic acid was produced by aerobic fermentation of ethanol, in fact it is still the main process for the production of vinegar. For the synthetic production, the oxidation of acetaldehyde was the first main commercial process of acetic acid. In Germany 1916, early introduced process may the conversion of acetylene to acetaldehyde. Recently, China still used an oregano mercury compound as the catalyst. However, because of the toxicity of the mercury catalyst resulted in significant environmental pollution. In addition, acetic acid can be produced by aerobic and anaerobic fermentation [11]. In the 1950s, the production raw material of acetaldehyde changed to ethylene, especially after petrochemical industry developed. By 1950s and 1960s, other production processes of acetic acid introduced, where most of it was based on the oxidation of naphtha and n-butane. In addition, significant amounts of oxidation by-products are produced by those reactions and their separation process and recovery can be very complex and expensive, more details in Table 2.2 [12].

Table 2.2: Processes of acetic acid production [12].

	Catalyst	**Reaction condition (°C, atm)**	**Yield**	**By-product**
Methanol carbonylation	Rhodium complex	180–220, 30–40	MeOH: 99%, CO: 85%	----
Acetaldehyde oxidation	Manganese acetate or cobalt acetate	50–60, atmospheric pressure	CH_3CHO: 95%	----
Ethylene direct oxidation	Palladium/ heteropolyacid / Metal	150–160, 80	Ethylene: 87%	Acetaldehyde CO_2
Hydrocarbon oxidation (*n*-butane, naphtha)	Cobalt acetate or manganese acetate	150–230, 50–60	*n*-Butane: 50%, naphtha: 40%	Formic acid, propionic acid, etc

The methanol carbonylation technology has been used for all new acetic acid production. That technology was developed by Monsanto and practiced commercially by all major acetic acid manufacturers, including BP-Amoco, Celanese, and others. Figure 2.2 shows that more than 60% of the world acetic acid production employs the methanol carbonylation methods.

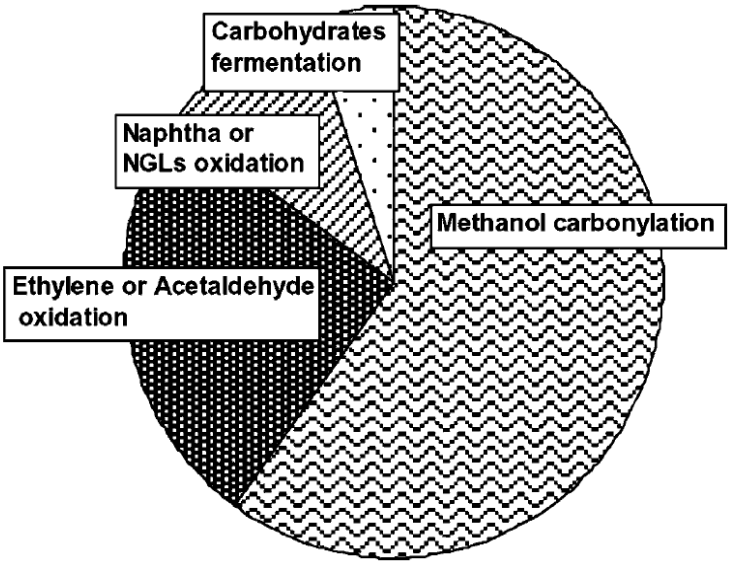

Figure 2.2: The routes of acetic acid process [12].

Mainly in industry sector, the acetic acid produced from methanol carbonylation and acetaldehyde oxidation. Unfortunately, that rise to many problems concerning handling, waste disposal or corrosion [13].

2.1.2.1 Methanol carbonylation

1. The Rhodium Based Monsanto Process

Acetic acid produced by Monsanto process, which used a rhodium catalyst. The process conditions were, the temperatures in between 150 to 200°C, and pressure in between 30 to 60 atmospheres. In addition, methanol was over then 99% for the main feed stock, At Monsanto, Forster and his co-workers has investigated this reaction and accepted the mechanism. With six discrete and interlinked reactions, the cycle is a classic example of a homogeneous catalytic process [14, 15].

Methyl iodide generated during the methanol carbonylation by the reaction of adding hydrogen iodide to methanol [14]. Figure 2.3 shows the main units comprising a commercial scale Monsanto methanol carbonylation plant. The Monsanto methanol operating plant is the main unit comprising a commercial-scale that utilizing rhodium based catalyst. Three distillation columns are used in this technique to deliver high purity acetic acid product by sequentially retinae low boilers (methyl iodide and tenthly acetate) as well as water and high boilers (propionic acid).

The methyl iodide is provided by the reaction of feed methanol with hydrogen iodide, equation 2.1 [12]:

$$CH_3OH + CO \rightarrow CH_3COOH \qquad 2.1$$

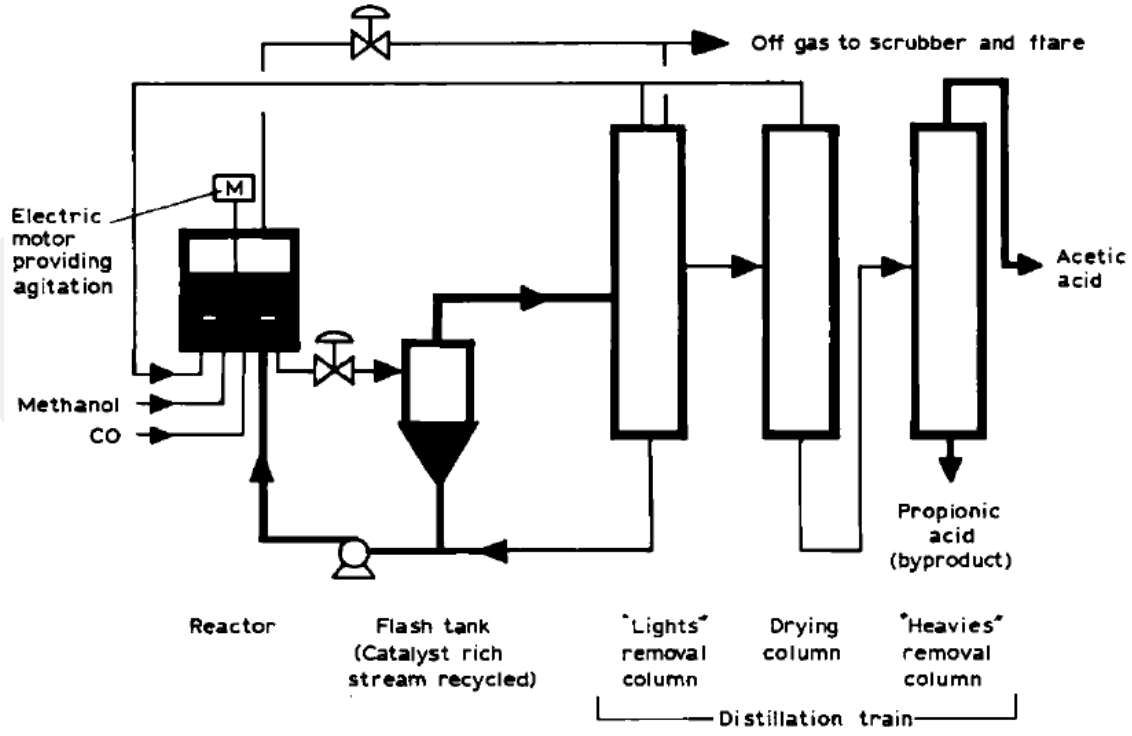

Figure 2.3: The operating plant Monsanto methanol [14].

2.1.2.2 Ethylene Oxidation

The acetic acid production by ethylene oxidation process contains two-step, which start from ethylene through acetaldehyde. In fact, it was the first used. Equations 2.2 and 2.3 show the reactions [12]:

$$CH_2=CH_2 + ½\ O_2 \rightarrow CH_3CHO \quad (2.2)$$

$$CH_3CHO + ½\ O_2 \rightarrow CH_3COOH \quad (2.3)$$

Liquid phase of acetaldehyde oxides utilized air, and normally with a manganese acetate catalyst operating at 50–60 °C. In fact, this process features with high yield approximately 90% as well as relatively low cost. However, it suffers from high corrosive catalyst unit and high acetaldehyde feedstock cost.

2.1.2.3 Other production technologies

1. Ethane oxidation

The use of ethane to produce acetic acid was first done in the 1980s. That process is done with two reaction mechanisms, which based on equation 2.4:

$$CH_3CH_3 + O_2 \rightarrow CH_3COOH + \text{by-product} \quad (2.4)$$

Several catalyst systems were suggested:

- The methyl group partial oxidation
- Ethane oxidation to ethylene followed by ethylene hydration to ethanol, or ethylene to acetaldehyde.

Reacting ethylene, ethane or mixtures of ethylene and ethane with oxygen can produce the acetic acid over a catalyst containing molybdenum or vanadium, and one other metal. In addition, next reaction showing the hydration route, which is combined ethane or ethylene in feed case, the hydration catalyst further catalyzes the hydration of ethylene to ethanol that lead to produced acetic acid.

$$CH_2=CH_2 + H_2O \rightarrow CH_3CH_2OH \quad (2.5)$$

$$CH_3CH_2OH + O_2 \rightarrow CH_3COOH + H_2O \quad (2.6)$$

Catalyst: Pd-H_3PO_4/SiO_2

The second reaction shows the partial oxidation route and the oxidation reaction of catalyst catalyzes ethylene to acetic acid as well as other oxidation products, which produces acetic acid [8].

$$CH_2=CH_2 + ½\ O_2 \rightarrow CH_3CHO \quad (2.7)$$

$$CH_3CHO + ½\ O_2 \rightarrow CH_3COOH + H_2O \quad (2.8)$$

Catalyst: Pd-V_2O_5, Pd-V_2O_5-Sb_2O_5 /SiO_2

In addition, Ethylene concentration was kept below 3%. If it above 3% then there is always possibilities of formation such products of acetaldehyde, ethanol etc. as a consequence, the yield of acetic acid was lowered.

(Main reaction) $C_2H_4 + O_2 \rightarrow CH_3COOH$ 2.9

(Side reactions) $C_2H_4 + 3O_2 \rightarrow 2CO_2 + 2H_2O$ 2.10

$C_2H_4 + (^1/_2)\ O_2 \rightarrow CH_3CHO$ 2.11

2. Methane carbonylation

Directly from methane, acetic acid production under relatively mild conditions has been reported. In the presence of $Pd(OCOCH_3)_2$ / $Cu(OCOCH_3)_2$/ $K_2S_2O_8$ / CF_3COOH, acetic acid can be produced from methane and carbon monoxide. In addition, with presence of rhodium dichloride dissolved in water, acetic acid producing by the mixture of methane, carbon monoxide and oxygen:

$CH_4 + CO + ½\ O_2 \rightarrow CH_3COOH$ 2.12

With a high yield of acetic acid, this reaction proceeds in an aqueous medium at a temperature of nearly 100 °C [12].

2.2 ACETIC ACID PRODUCTION BY OXIDATION OF ETHYLENE

Some researchers developed a one-stage process for acetic acid production through the gas-phase oxidation of ethylene. The reaction path of production acetic acid, by hydration of ethylene to ethanol on the acid sites, then oxidation to acetaldehyde and finally producing acetic acid [16].

2.2.1 Direct Oxidation Process Using Air

Before mixing air with fresh ethylene, should first be purified to remove contaminants from air and then compressed to mix with recycled gas to ethylene. In addition, some components like ethylene dichloride or vinyl chloride added in the inlet of the reactor to retard carbon dioxide formation in vapor phase oxidation [17]. During gas feeding to a catalytic reactor, the operation temperature is controlled by boiling water in other cases with circulated non-boiling organic oil on the shell side, while oil is utilizing, the cooling in a steam generator, which is producing high pressure steam that benefit in the process.

After reactor, the effluent gas that contains ethylene oxide is cooled in heat exchanger with cold reactor feed gas. The main absorber or cooled gas produced a dilute aqueous solution, then the ethylene oxide is absorbed in water. From the absorber, the scrubbed gas is compressed to recycle to the main reactor.

2.2.2 Direct Oxidation Process with Oxygen

With recycled gas the fresh ethylene is mixed with high purity oxygen, these mixtures are the fed into reactor. Before enters to absorber, the effluent gas that contains

ethylene oxide deals with cold reactor fed gas in heat exchanged. In addition, dilute aqueous solution is produced in the absorber, when ethylene oxide is dissolved in the absorber water. Then gas is scrubbed in the reactor by compressed and recycled. As a part of operation, the recycle gas is first sent to a CO_2 absorber. In the reactor, carbon dioxide produced by chemically absorbed in a recirculated solution by hot potassium carbonate.

After that, the CO_2 gas is returned to the recycled gas to the reactor. CO_2 rich carbonate solution is regenerated in the CO_2 stripper utilizing stream and the desorbed carbon dioxide is vented out in the top of the column.

2.2.3 Absorption

Absorption, it is an operation that accrues when two phases gas and liquid are contacting, by solute from the gas phase into the liquid phase in absorption [7]. Normally, the absorption is based on reactions between CO_2, and one or more basic absorbents. An advantageous feature of absorption, it can be reversed, the temperature is raised by sending the CO_2,-rich absorbent to stripper. In other case of CO_2 absorption, under pressure the gas desorption can be achieved at decreasing pressure, with continuous recycling process, the regenerated absorbent is returned to the absorber [18]. Acetic acid can be recovered by absorption even at low concentrations. In fact, the absorption classified into two main types: physical absorption (non-reactive) and reactive absorption.

Physical absorption: This process refers to the process that occurs at the interface between specific gas or mixture of gasses and liquid regarding to the diffusion of gas or gasses in the liquid. In turn, mentioned process controlled by some parameters such as,

gas solubility, pressure and temperature. Production of ammonia by absorption in water is the best example.

Reactive (Chemical) absorption: This process differs from one mentioned above in chemical reactions that occur between components. Reaction stoichiometry and substances concentrations are the main variable of the process. Main advantages are larger solution capacity, moderate application pressure and enhanced selectivity [19]. This process considers as a core of most separation techniques in chemical industries addition to product of essential chemicals such as nitric and sulphuric acid [20].

2.3 THEORY

Using ethylene oxidation method to produce acetic acid method, all of work will be done by simulating the absorption process using ASPEN PLUS. The effect of various parameters as pressure, temperature, flow rate and number of theoretical stages will be studied and modeled.

Based on that, the production process design of acetic acid by utilized carbon dioxide needs three stages, which are reaction and separation and gas scrubber:

1. Reactor
2. Flash drum
3. Absorber or scrubber

2.3.1 None Random Two Liquid NRTL Model

Renon and Prausnitz developed the none random two liquid, which also known as NRTL equation [21, 22]. None random two liquid equation is applicable to multicomponent liquid-liquid and vapor-liquid, as well as vapor-liquid-liquid systems. Such a case of multicomponent vapor-liquid systems, only binary-pair constants from the corresponding binary-pair experimental data are required. The NRTL expression for the activity coefficient for a multicomponent system as following [22]:

$$ln\gamma_i = \frac{\sum_{j=1}^{C} \tau_{ji} G_{ji} x_j}{\sum_{k=1}^{C} G_{ki} x_k} + \sum_{g=1}^{C} \left[\frac{x_g G_{ij}}{\sum_{k=1}^{C} G_{kj} x_k} \left(\tau_{ij} - \frac{\sum_{k=1}^{C} x_k \tau_{kj} G_{kj}}{\sum_{k=1}^{C} G_{kj} x_k} \right) \right] \quad 2.13$$

Where:

$$G_{ji} = \exp(-\alpha_{ji} \tau_{ji})$$

The coefficients τ are given by

$$\tau_{ij} = \frac{g_{ij} - g_{ij}}{RT}$$

$$\tau_{ji} = \frac{g_{ji} - g_{ji}}{RT}$$

.

2.3.2 Absorption Factor

According to J. D. Seader 2006, the fraction of a component that can be absorbed or stripped in a countercurrent cascade depends on the number of equilibrium stages and the absorption factor [22]:

Absorption Factor = $\frac{L}{KV}$

Where:

L: average liquid rate

V: average vapor rate

K: is the fraction

Generally, if A values is more than 1, that mean any degree of absorption can be achieved, where

- The larger value of A: that mean required a fewer number of stages to absorb a desired fraction of the solute.
- Large values of A: can correspond to absorbent flow rates that are larger than necessary.

Economically, the A value must be in the range of 1.25 to 2.0, where recommended value within 1.4 [21-23].

$$k = \frac{Y}{X}$$

Where:

Y: is the mole fraction of vapor phase

X: is the mole fraction of liquid phase

$$k = \frac{0.984x0.003 + 1.27x10^{-16} + 0.012}{0.005 + 0.99 + 0.004 + 1.35x10^{-6}}$$

$$k = 1$$

$$A = \frac{L}{VK} = \frac{151.078\frac{kmol}{hr}}{98.921x1\frac{kmol}{hr}}$$

$$A = 1.527$$

No. of stages = 6

Actually, different catalysts and a wide range of temperature degrees applied at low fixed pressure reported increase in selectivity of acetic acid product [21].

2.3.3 Henry's law

William Henry in 1803 has formed the Henry's law. Henry's law say, that the amount of a given gas that dissolves in a given type and volume of liquid is directly proportional to the partial pressure of that gas in equilibrium with that liquid at a constant temperature [24].

The solubility of a gas in a liquid is the key, where directly proportional to the partial pressure of the gas above the liquid as shown in formula [25-27]:

$$C = kP_{gas}$$

Where

C: is the solubility of a gas at a fixed temperature

k: is Henry's law constant

P_{gas} : is the partial pressure of the gas

2.4 ASPEN PLUS

The name of ASPEN is Advanced System for Process Engineering. The MIT's Energy Laboratory researchers developed in 1970s a prototype for process simulation. In

1980's, ASPEN software has been commercialized, that foundation by company named Aspen Tech. In chemical process industries, ASPEN PLUS offers a complete integrated solution. In all aspect of process engineering, ASPEN software package can be used, which started from design stage to cost and profitability analysis [28-30].

Using FORTRAN subroutines and Excel worksheets, the user models are created. In thermodynamic and physical parameters, property databank can be built [31]. Aspen Plus estimates any missing parameter automatically during the calculation of the flow sheet, by several group contribution methods. In fact, Aspen Plus can estimate many tasks like generating custom graphical and output results, regressing physical properties, fitting plant data to simulation models, optimizing process, and interfacing results to spreadsheets. The specifications like flow sheet configuration, operating conditions, and feed compositions, can be interactively changed to run new cases and analyze process alternatives by Aspen Plus [32].

CHAPTER 3

MODELING

3.1 PRODUCTION PROCESS

The production model is designed with three stages; all stages have particular functions. Stage one is plug flow reactor, stage two is flash drum and last stage is RadFrac absorption or scrubber unit. Third stage is the main stage in this research. Figure 3.1 shows process flow diagram.

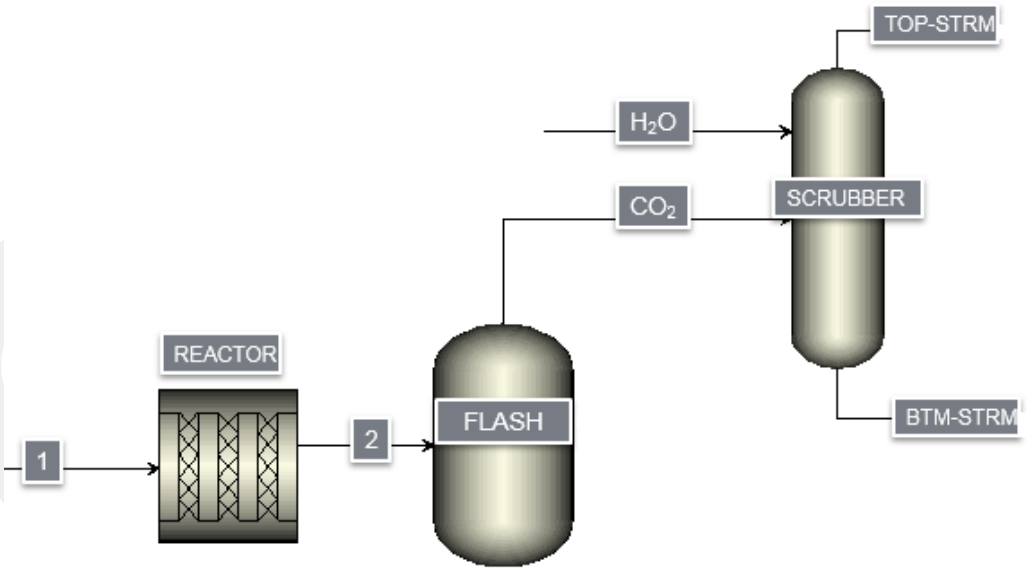

Figure 3.1: Main flow sheet for the modeling process.

3.2 PRODUCTION MODEL

3.2.1 Plug Flow Reactor

Plug flow reactor is first stage in acetic acid production model, in this reactor two reactions have taken place as in Equations 3.1 and 3.2. The input to the reactor was air and ethylene; these reacted at a special temperature and pressure, 250 °C and 20 bar respectively, as shown in Table 3.1. In addition, the reactor output was used as input in second stage. The plug flow reactor temperature was 250 °C and pressure was 20 bar, where reactor input divided to 30 wt% air and 70 wt% ethylene, while the output contains CH_3COOH with 89.9 wt% which is the highest percentage, CO_2 with 7.2 wt% and the lowest value was H_2O with 2.9 wt%. It should be mentioned that the feedstock to the reactor were air and ethylene where the ratio was 30 wt% air and 70 wt% ethylene. Nitrogen is essential element of air and does not have any effect on the reaction as it known as inert gas. In present equation, the ratio of N is small (traces).

$$C_2H_4 + Air \rightarrow CH_3COOH \quad (3.1)$$

$$C_2H_4 + Air \rightarrow CO_2 + H_2O \quad (3.2)$$

$$Yield\ Percent = \frac{theoretical\ yield\ of\ product}{actual\ yield\ of\ product} x\ 100$$

For first reaction at equation (3-1):

Theoretical yield = 150

Actual yield = 36.31

Percent yield = 24.20 %

For second reaction at equation (3-2):

Theoretical yield =110

Actual yield = 36.10

Percent yield = 32.81%

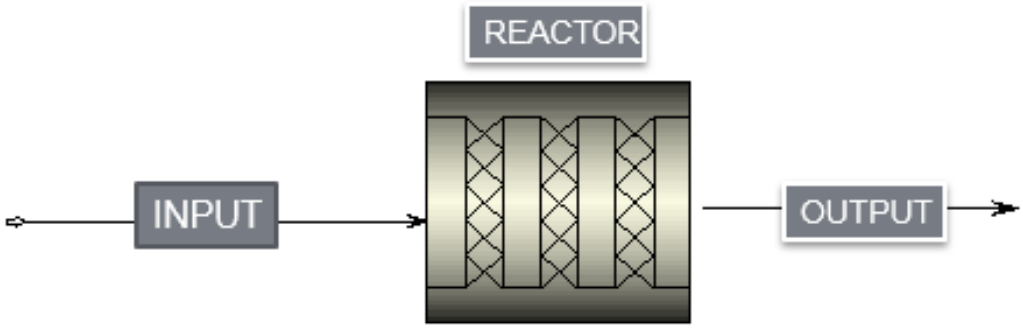

Figure 3.2: Stage 1, the reactor plug flow reactor.

Table 3.1: Stage 1, Plug flow reactor input and output.

TEMPERATURE °C	**PRESSURE** bar	**INPUT** wt%		**OUTPUT** wt%	
250	20	Air	30	CH_3COOH	89.9
		Ethylene	70	CO_2	7.2
				H_2O	2.9

3.2.2 Flash Drum

The second stage is the flash drum, as seen in Figure 3.3. This stage that utilizes the reactor output as input. More details about input and output are shown in Table 3.2. CO_2 was produced from this stage used as input in Radfrac absorber to produce acetic acid. The input of flash drum contains the output of plug flow reactor, which are CH_3COOH with 89.9 wt% which is the highest percentage, CO_2 with 7.2 wt% and the lowest value was H_2O with 2.9 wt%, while the flash drum output are divided as CH_3COOH with 0.6 wt%, CO_2 with 98.2 which the highest percentages and N_2 with 1.2 wt%.

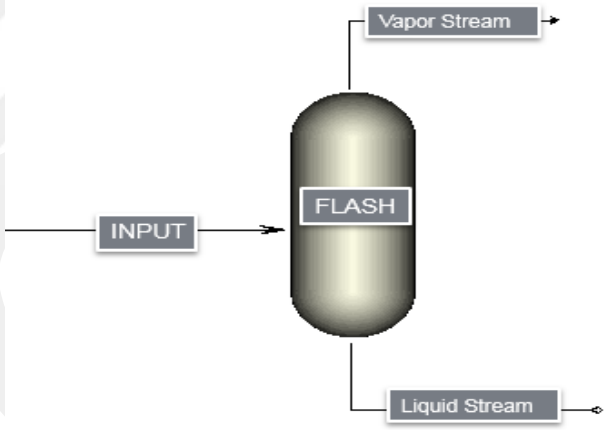

Figure 3.3: Stage 2, Flash drum.

Table 3.2: Stage 2, Flash unit input and output.

INPUT wt%		**OUTPUT** wt %	
CH_3COOH	89.9	CH_3COOH	0.6
CO_2	7.1	CO_2	98.2
H_2O	2.9	N_2	1.2

3.2.3 RadFrac scrubber

In stage 3, the RadFrac absorption or scrubber unit was designed to produce the largest possible amount of acetic acid. As rigorous model, the RadFrac is useful for to simulating all types of multistage vapor liquid fractionation processes. In fact, it can simulate:

- Absorption
- Stripping

In addition, RadFrac can be utilized with different kinetics for two liquid phases, as well as the model columns with two liquid phases chemical absorption in each liquid phase occurring simultaneously. RadFrac consists of trays used with especial size and rate columns. Moreover, it is the largest and most important stage of equipment in an acetic acid plant. RadFrac can treat large volume of flue gas. In this stage, the absorber column was designed based on equilibrium principles using the model data, which was created by using ASPEN Plus, as shown in Figure 3.4. Table 3.3 shows the Radfrac input, CO_2 and H_2O of this unit, where the stage flow rate , temperature and pressure has been shown. All inputs absorbed within 6 stages inside Radfrac. Acetic acid was produced in bottom stream as liquid. The flow rate, temperature and pressure have been controlled and sensitivity analysis was preformed as well on the process production.

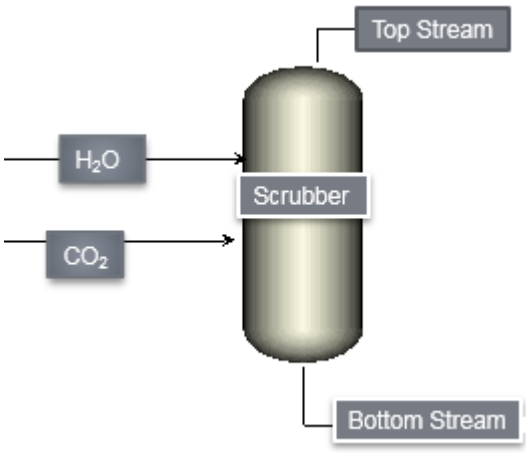

Figure 3.4: Stage 3, Radfrac scrubber.

Scrubber designed to control gaseous emissions and work on avoiding some unwanted gasses through exhaust streams. In current system water was used, the choice actually depends on the concentration of acetic acid inter the scrubber and somehow on the efficiency of gas removing. In case of low flow where the pollutants release frequently, water scrubber success to eliminate toxin. Moreover, when acetic acid produce at heavier amounts the better instead method is distillation column or a recirculated alkali solution.

Other than water, the following can be used as liquid absorbent: carbon tetrachloride, ether, ethyl alcohol and glycerol. However, using (NaOH) which considers as strong base to absorb acetic acid leads to produce sodium cations and hydroxide anions as it is totally dissociated in aqueous solution. Sodium acetate is produced because of this reaction. Similarly, sodium acetate soluble and in turn exist as ions.

Table 3.3: Stage 3, Radfrac input and output.

	H_2O stream		**CO_2 stream**	
	INPUT			
FLOW RATE kmol/hr	150		100	
TEMPERATURE ^{O}C	25		40	
PRESSURE bar	10		10	
Composition wt%	Water	150	CO_2	98.2
			CH_3COOH	0.6
			N_2	1.2

3.3 SENSITIVITY ANALYSIS

Sensitivity analysis allows to study and evaluate the effect of input variables and their changes in process outputs. The sensitivity results can be reviewed in the next chapter in the sensitivity part. Generally, the sensitivity simulation runs independently of the production simulation. Any changes made to process input quantity in sensitivity part do not affect the production simulation. In this production simulation, the sensitivity analysis deals with temperature and pressure. In ASPEN Plus model multiple inputs can be varied. Then the simulation model should be run for every combination of manipulated variables. In this study, sensitivity has been analyzed to both CO_2 and H_2O stream as seen in

Figure3.5. this sensitivity analysis has been focused on temperature , pressure and flow rate as operational parameters.

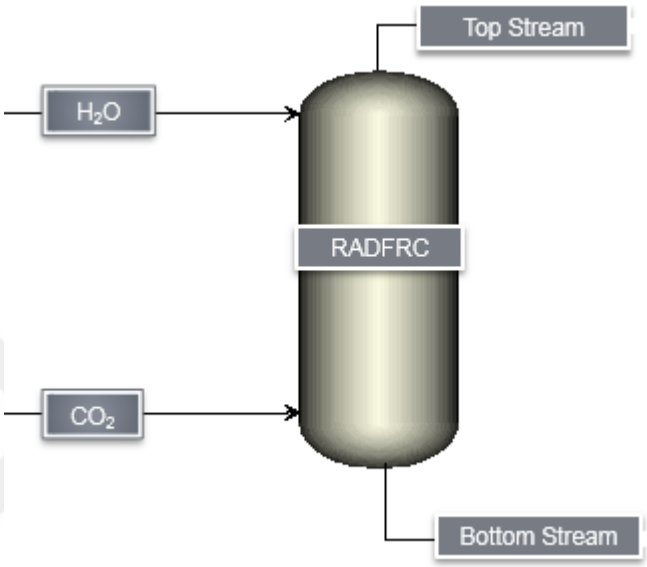

Figure 3.5: The process streams of scrubber for sensitivity analysis.

3.3.1 Sensitivity Analysis of CO_2 Stream

3.3.1.1 Effect of CO_2 Stream Flow rate

The effect of CO_2 flow rate as input in the RadFrac absorption (scrubber) unit has been measured by sensitivity analysis. The effect of CO_2 flow rate on overall Radfrac unit production has been analyzed. This sensitivity has been analyzed by sensitivity tool in Aspen Plus, a new sensitivity added variable 1 in simulation model and that new variable is selected as Stream-Variable and the stream was to be CO_2. The manipulation will be in total flow rate in kmol/hr of the feed stream to the Radfrac. In addition, the start point has

been selected as 80 kmol/hr and the end point was 500 kmol/hr as shown in Figure 3.6. The sensitivity increment variables has been recorded at every 20 kmol/hr.

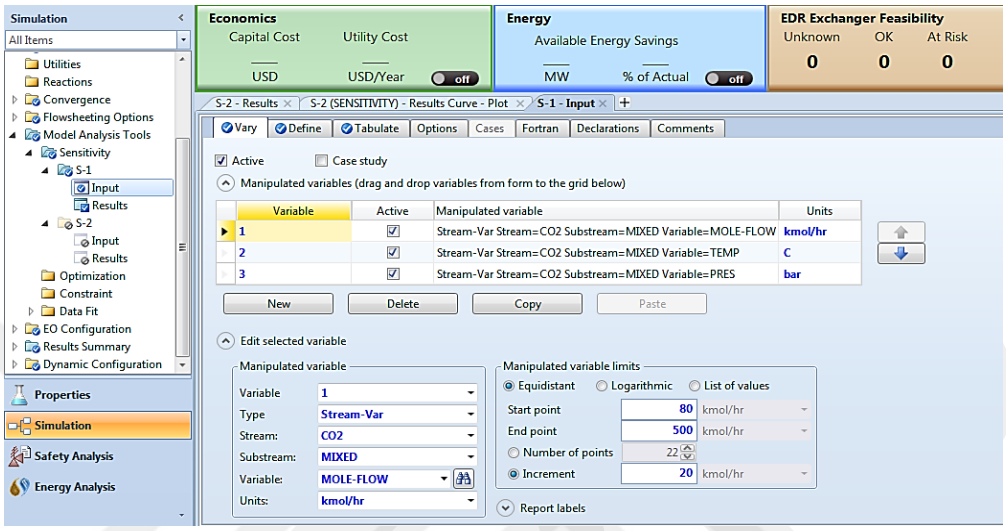

Figure 3.6: The sensitivity setup of CO_2 flow rate as manipulated variable.

3.3.1.2 Effect of CO_2 Stream Temperature

The aim of sensitivity analysis based on temperature of the CO_2 input to the RadFrac absorption (scrubber) unit is to find out the effect of CO_2 temperature on Radfrac unit production. This sensitivity has been analyzed by sensitivity tool in Aspen Plus. A new sensitivity was added as variable 2 in simulation model, that new variable is selected as Stream-Variable, and the stream was to be CO_2. That means the manipulation will be in the temperature °C of the feed stream to the Radfrac. In addition, the start point has been selected as 40 °C and the end point was 80 °C as shown in Figure 3.7. The increment of the sensitivity variables has been recorded for every 5 °C of temperature.

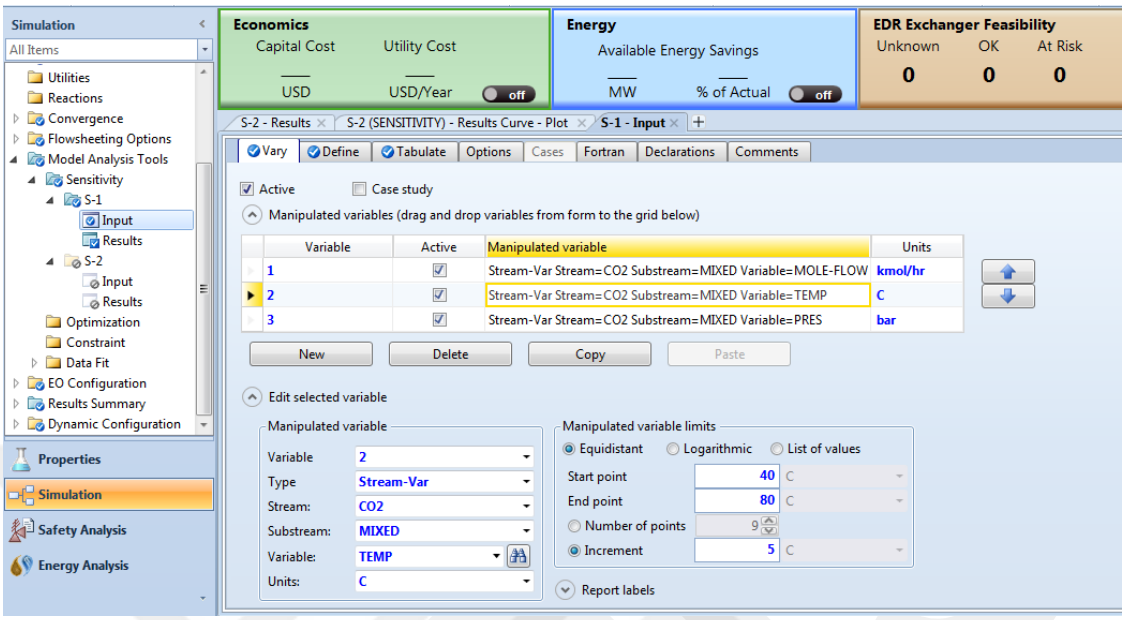

Figure 3.7: Sensitivity setup of CO_2 temperature as manipulated variable.

3.3.1.3 Effect of CO_2 Stream Pressure

This sensitivity analysis aims to analyze the effect of the pressure of CO_2 input stream to the RadFrac absorption or scrubber unit on acetic acid production as well as the effect of CO_2 pressure on the overall production. A new sensitivity was added as variable 3 in simulation model and that new variable is select the type as Stream-Variable and the stream to be CO_2. Manipulation will be in total pressure of the feed stream of the Radfrac. In addition, the start point of variable limits has been selected as 10 bar and the end point was 100 bar as shown in Figure 3.8. The increment of the sensitivity variables has been recorded for every 10 bar.

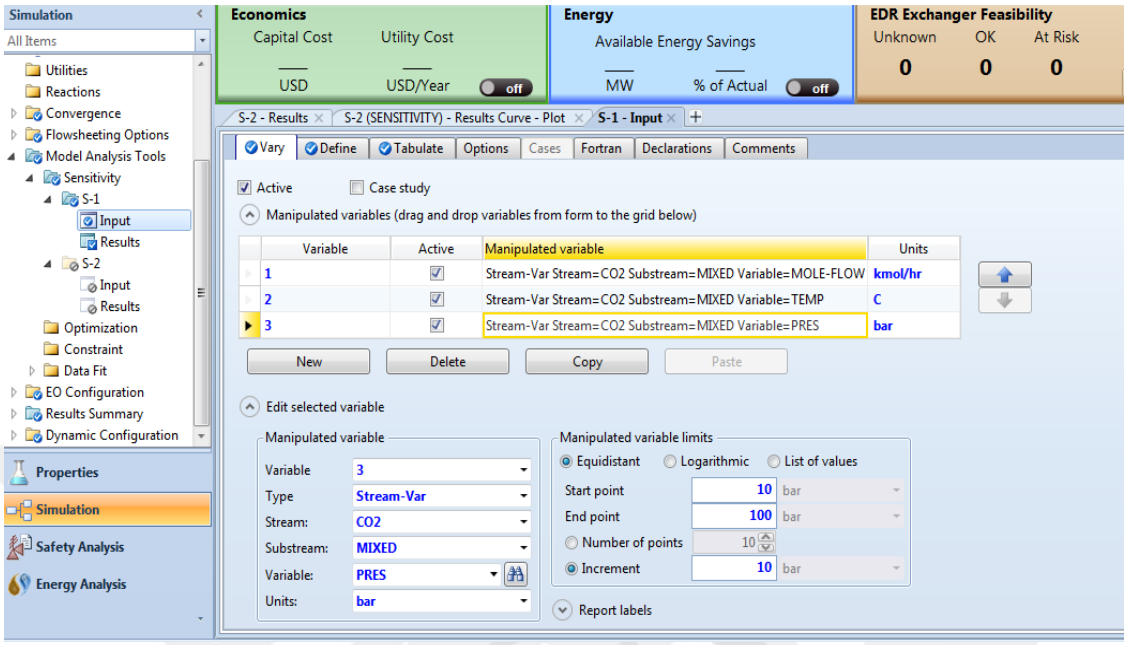

Figure 3.8: Sensitivity setup of CO_2 pressure as manipulated variable.

3.3.2 Sensitivity Analysis of H_2O Stream

3.3.2.1 Effect of H_2O Stream flow rate

Here, the sensitivity analysis of H_2O flow rate has been studied. The H_2O input stream in the scrubber unit has been measured by sensitivity analysis. The effect of H_2O flow rate on the overall production was aimed to find out. The sensitivity tool in Aspen Plus was utilized in this model. A new sensitivity was added as variable 1 in simulation model and that new variable is selected the type as Stream-Variable and the stream to be H_2O. Here, manipulation will be in total flow rate with kmol/hr of the feed stream to the Radfrac. As shown in Figure 3.9 the start point has been selected as 30 kmol/hr and the end point was 150 kmol/hr. In addition, the sensitivity increment variables has been recorded every 10 kmol/hr.

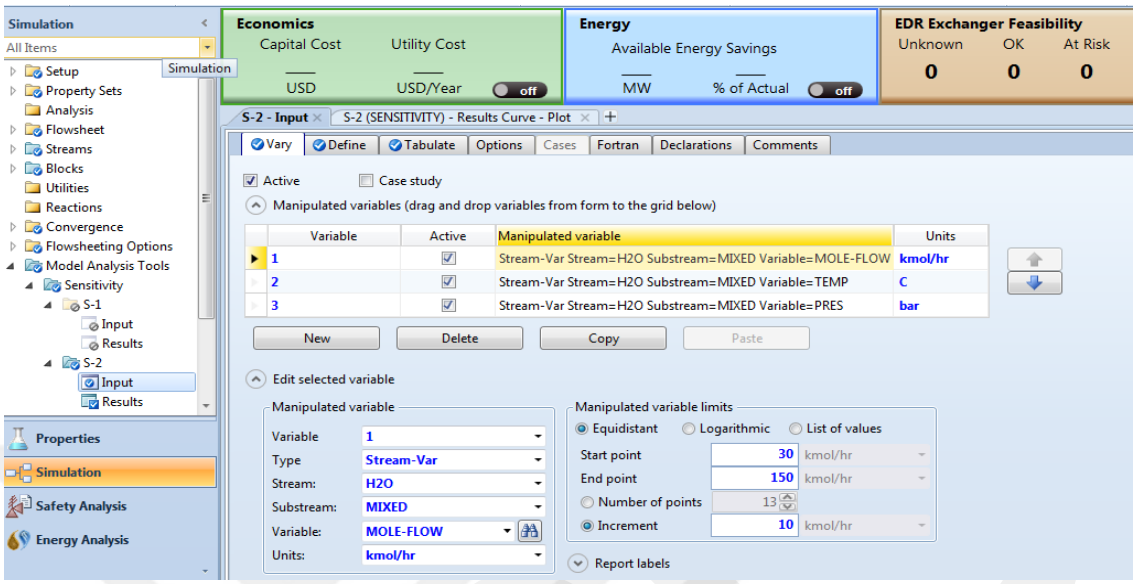

Figure 3.9: The sensitivity analysis setup of H_2O flow rate as manipulation variable.

3.3.2.2 Effect of H_2O Stream Temperature

Here, it is aimed to find out the effect of H_2O stream temperature on Radfrac unit production. This sensitivity analysis has been preformed by sensitivity tool in Aspen Plus. A new sensitivity was added as variable 2 in simulation model and that new variable was selected the type as Stream-Variable and the stream to be H_2O. Manipulation will be in total temperature of the feed stream to the Radfrac unit. In addition, the start point has been selected as 25 °C and the end point was 100 °C as shown in Figure 3.10. The increment of the sensitivity variables has been recorded every 5°C.

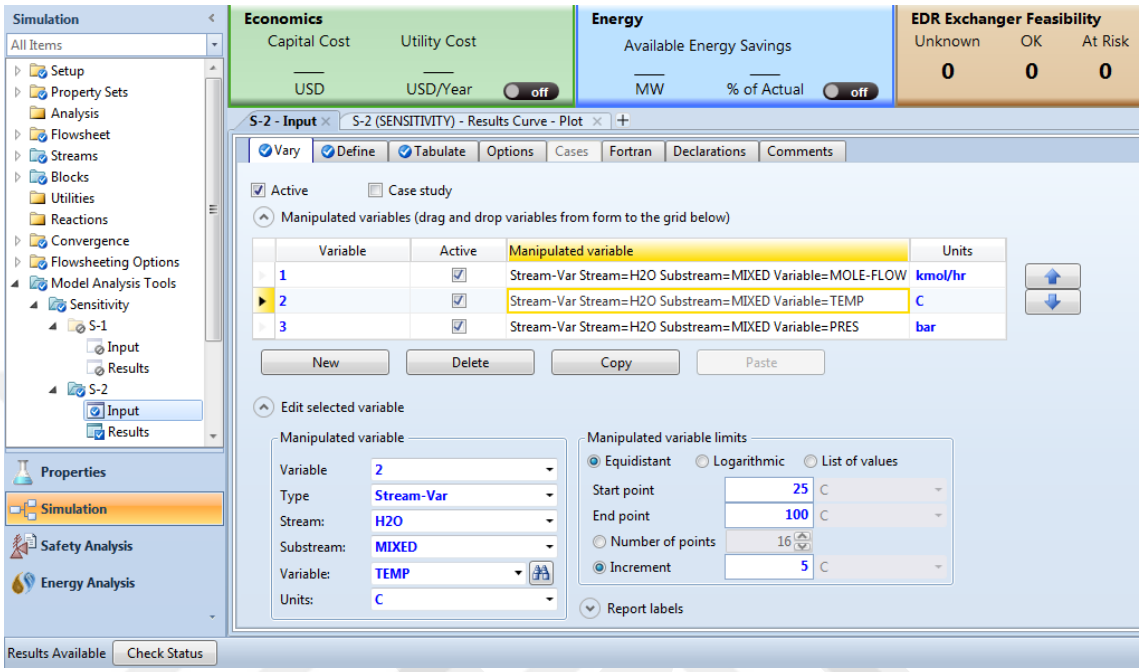

Figure 3.10: The sensitivity analysis setup of H_2O stream temperature as manipulation variable.

3.3.2.2 Effect of H_2O Stream Pressure

Similarly to the sensitivity analysis of temperature, the main aim of sensitivity analysis of H_2O pressure is to study the effect of H_2O input stream to the scrubber unit on acetic acid production as well as to find out the effect of H_2O pressure on overall Radfrac unit production. A new sensitivity was added as variable 3 in simulation model and that new variable was selected the type as Stream-Variable and the stream to be H_2O. Manipulation is made in total pressure with bar of the feed stream to the Radfrac. In addition, the start point has been selected as 10 bar and the end point was 80 bar as shown in Figure 3.11. The increment of the sensitivity variables has been recorded at every 10 bar.

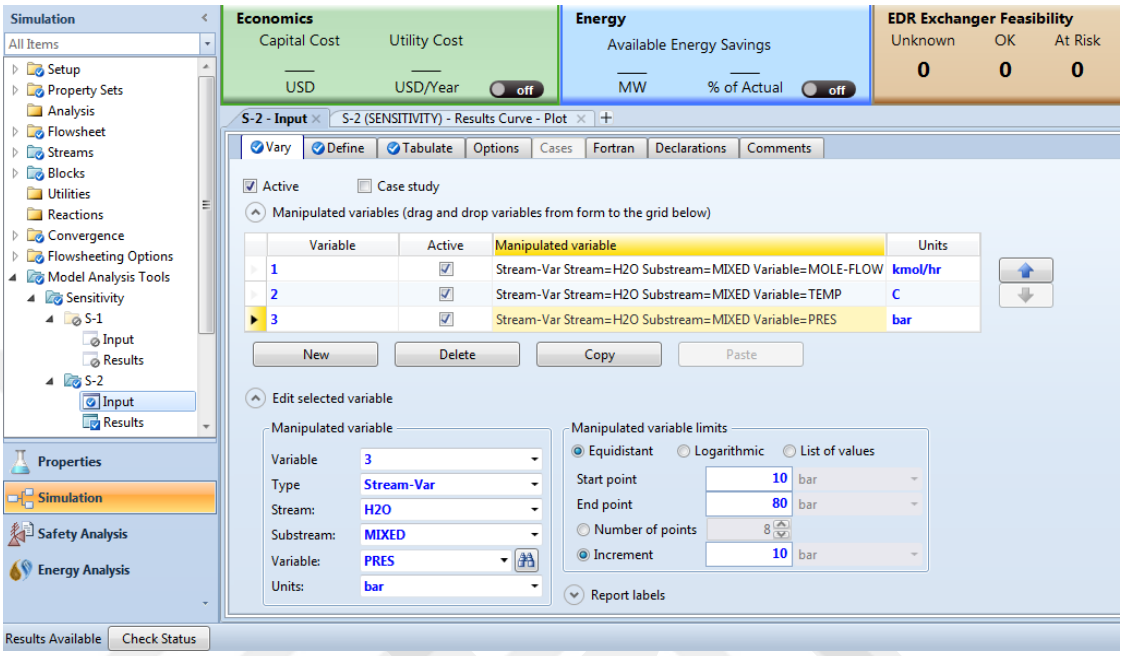

Figure 3.11: The sensitivity analysis setup of H_2O pressure as manipulation variable.

CHAPTER 4

RESULTS AND DISCUSSIONS

4.1 PRODUCTION BY SCRUBBER

The main stage of our modeling design is the third stage, which is the RadFrac scrubber unit. This unit has been designed to produce the largest possible amount of acetic acid and produce CO_2 as pure as possible. Moreover, RadFrac represented as the largest and most important stage of equipment in an acetic acid plant. Figure 4.1 shows the third stage which is the absorber column based on equilibrium principles using the model data in simulation software. Acetic acid has been produced as liquid in the bottom stream using six stages because the absorption factor is high according to liquid feed height inside Radfrac. In addition, the flow rate, temperature and pressure have been controlled and analyzed as sensitivity parameters.

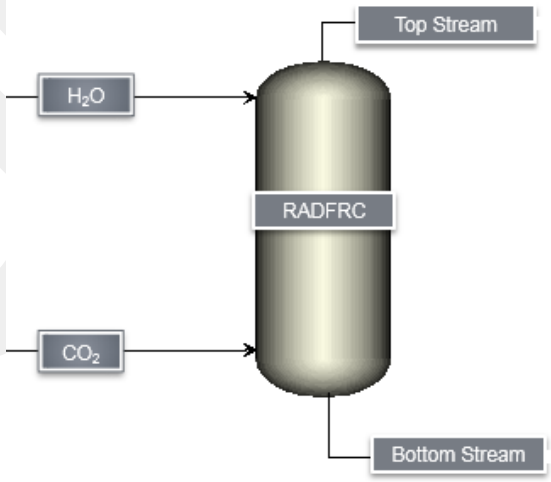

Figure 4.1: The input and output of third stage.

Table 4.1 shows the mole flow of input and output of the scrubber. CO_2 stream bottom input with 98.2 kmol/hr total mole flow at 40 °C temperature and 10 bar pressure. The top input was H_2O stream with a mole flow of about 150 kmol/hr, at 25 °C temperature and as same as CO_2 stream pressure 10 bar. The basic product is acetic acid, which is produced in the bottom stream with mole flow about 0.6 Kmol/hr, at 30.3 °C temperature and 10 bar pressure. The aim of this study scrub acetic acid at the Bottom stream. In addition, the separation process is excellent with the highest percentage of acetic acid at the bottom stream. Note that the proportion of CO_2 gas dissolved in water, because it is solve in water while nitrogen gas difficult to dissolve in water, for this reason most of the nitrogen gas flowed up as upper stream.

Table 4.1: Mole flows for all streams of the scrubber.

		BOTTOM INPUT	**TOP INPUT**	**BOTTOM PRODUCT**	**TOP PRODUCT**
Phase		Mixed	Liquid	Liquid	Vapor
Temperature	°C	40	25	30.3	26.5
Pressure	bar	10	10	10	10
Mole Flows	kmol/hr	100	150	151.078	98.921
CO_2	kmol/hr	98.2	0	0.820	97.379
H_2O	kmol/hr	0	150	149.657	0.342
CH_3COOH	kmol/hr	0.6	0	0.6	1.26 E-14
N_2	kmol/hr	1.20	0	0.0002	1.199

Table 4.2 shows the mole flow for RadFrac input and output. The RadFrac bottom input started with CO_2 at 0.982 kmol/hr mole fraction at 40 °C temperature and 10 bar pressure. The top input was H_2O with mole flow about 150 kmol/hr, at 25 °C temperature and 10 bar pressure. The basic product is acetic acid, which is produced as bottom stream with mole fraction of 0.004 at 30.3 °C temperature and 10 bar pressure and some of it as top stream nearly 1.27 E-16 kmol/hr at 26.571°C temperature and 10 bar pressure. In this study, we will recover acetic acid from diluted CO_2 mixture and that it is to make an almost pure CO_2 in this system. That concluded at top stream CO_2 at high purity. The purity of acetic acid was at the bottom stream is about 0.004 while in the top stream it is zero.

Table 4.2: The mole fractions for all streams of the scrubber.

		BOTTOM INPUT	**TOP INPUT**	**BOTTOM PRODUCT**	**TOP PRODUCT**
Phase		Mixed	Liquid	Liquid	Vapor
Temperature	°C	40	25	30.3	26.57
Pressure	bar	10	10	10	10
Mole Fractions	kmol/hr				
CO_2	kmol/hr	0.982	0	0.005	0.984
H_2O	kmol/hr	0	1	0.990	0.003
CH_3COOH	kmol/hr	0.006	0	0.004	1.27 E-16
N_2	kmol/hr	0.012	0	1.35 E-06	0.012

The mass flows of all streams are shown in Table 4.3 for RadFrac input and output. The mass flow of RadFrac bottom input started with CO_2 stream has a flow of 4321.762 kg/hr at 40 °C temperature and 10 bar pressure. The top input was H_2O stream with 2702.292kg/hr flow, 25 °C temperature and as same as CO_2 pressure 10 bar. The acetic acid produces as bottom stream with mass flow about 36.031 kg/hr, at 30.3 °C temperature and 10 bar pressure and some of it leaves as top stream at a rate of 7.57 E-13kg/hr, at 26.5 °C temperature and 10 bar pressure.

Table 4.3: The mass flows for all streams of the scrubber.

		BOTTOM INPUT	**TOP INPUT**	**BOTTOM PRODUCT**	**TOP PRODUCT**
Phase		Mixed	Liquid	Liquid	Vapor
Temperature	°C	40	25	30.3	26.5
Pressure	bar	10	10	10	10
Mass Flows	kg/hr	4391.410	2702.292	2768.264	4325.438
CO_2	kg/hr	4321.762	0	36.100	4285.662
H_2O	kg/hr	0	2702.292	2696.126	6.165
CH_3COOH	kg/hr	36.031	0	36.031	7.57 E-13
N_2	kg/hr	33.616	0	0.006	33.610

Table 4.4 shows the mass fraction for RadFrac stream input and output. The RadFrac bottom stream has a rate of CO_2 at 0.984 kg/hr mass flow at 40 °C temperature and 10 bar pressure. The top input was H_2O stream with mass flow about 1 kg/hr, 25 °C temperature and as same as CO_2 pressure 10 bar. The basic product is acetic acid, which produces as bottom stream with mass fraction about 0.013 kmol/hr, at 30.3 °C temperature and 10 bar pressure and some of it as top stream nearly 1.75 E-16 kmol/hr, at 26.5 °C temperature and 10 bar pressure.

Table 4.4: The mass fractions of all streams.

		BOTTOM INPUT	**TOP INPUT**	**BOTTOM PRODUCT**	**TOP PRODUCT**
Phase		Mixed	Liquid	Liquid	Vapor
Temperature	°C	40	25	30.325	26.571
Pressure	bar	10	10	10	10
Mass Fractions	kg/hr				
CO_2	kg/hr	0.984	0	0.013	0.990
H_2O	kg/hr	0	1	0.973	0.001
CH_3COOH	kg/hr	0.008	0	0.013	1.75 E-16
N_2	kg/hr	0.007	0	2.06 E-06	0.007

Table 4.5, which is available in the Appendices, shows the mole fraction for CH_3COOH with respect of every stage in RadFrac. These data displayed in Figure 4.2.

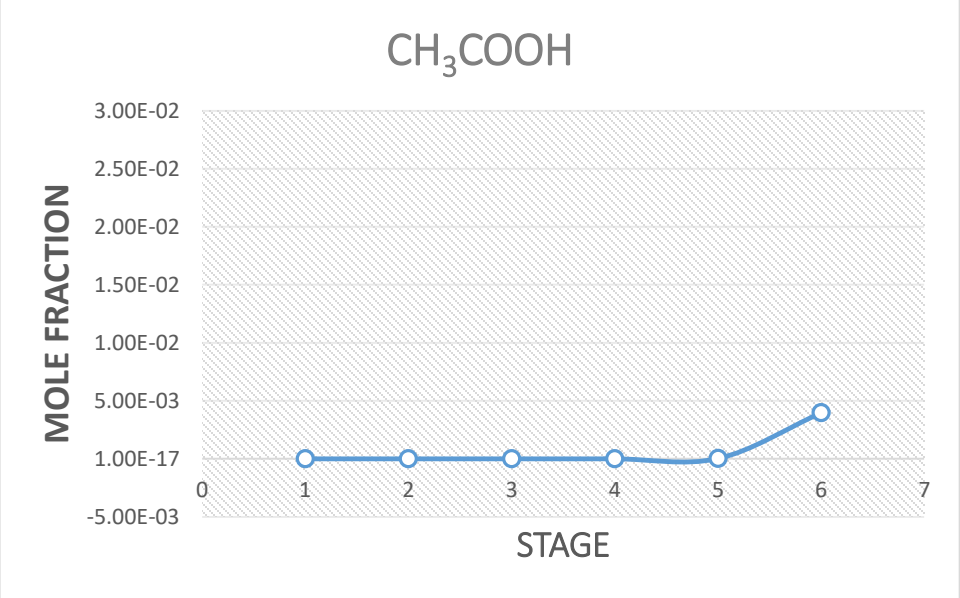

Figure 4.2: The liquid mole fraction of acetic acid at every stage.

Most of the acetic acid produced in the liquid phase, because molecules of the organic acid is non-volatile and interconnected that is why acetic acid gather at the last stage and exit the bottom stream.

The tiny amount of CO_2 resulted from conversion of acetic acid and this in turn refer to a small over-oxidation in air stream, and contribute in decrease of acetic acid production. It can overcome this problem by efficient aeration. In addition, by controlling the airflow of feedstock, which reduce air contact with ethylene and lead to prevent undesired gases to be exist.

4.2 SENSITIVITY ANALYSIS

4.2.1 Sensitivity Analysis of Acetic Acid Recovery

The main aim of this section is to modeling recovery of acetic acid by oxidation of ethylene with Aspen Plus. This part aims to find out the effect of various parameters such as the flow rate, temperature and pressure throughout RadFrac inputs CO_2 and H_2O on the bottom stream as shown in Figure 4.3. All the data regarding to the sensitivity analysis of acetic acid are shown in Tables 4.6 – 4.7, which are available in Appendices.

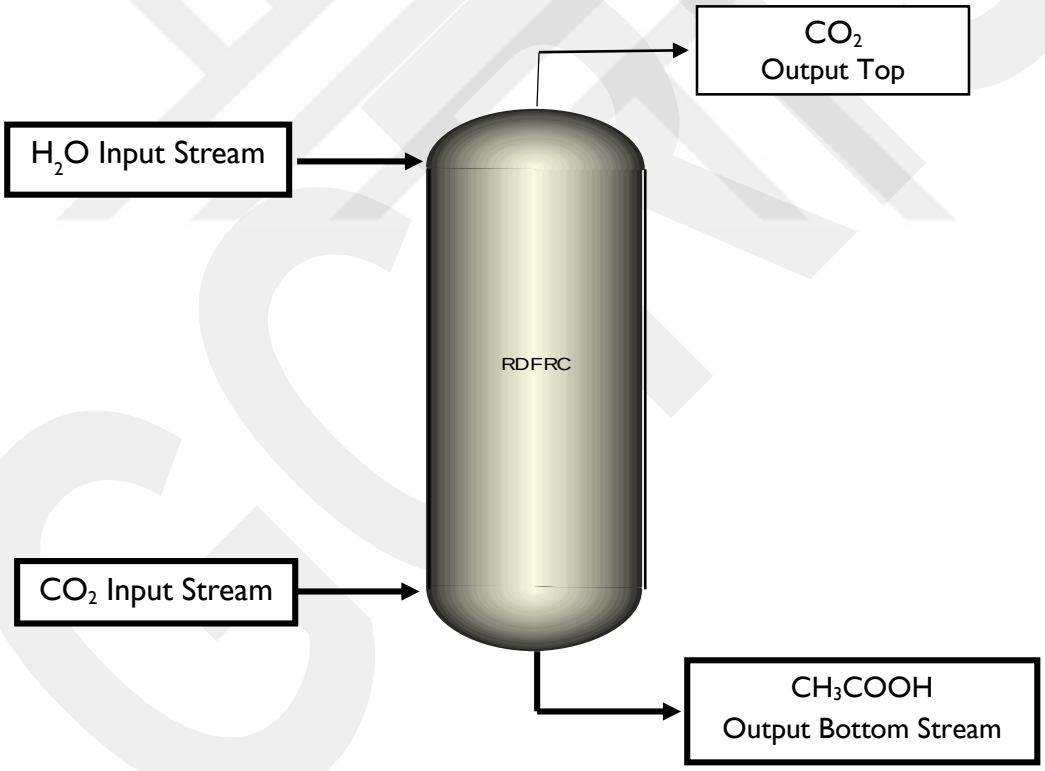

Figure 4.3: The RadFrac inputs in sensitivity analysis of acetic acid recovery.

4.2.1.1 The Sensitivity of H_2O Stream

1. **Effect of flow rate of inlet H_2O stream**

Figure 4.4 shows the effect of total mole flow with respect to temperature of H_2O on the mole fraction of CH_3COOH. The start point of mole flow was 15 kmol/hr and the end point was 200 kmol/hr. It was observed that increasing the flow rate of H_2O input stream decreases the mole fraction of CH_3COOH. The highest acetic acid mole fraction recorded was at start point. In addition, the effect of temperature was analyzed as well. The start point of temperature was 20 °C and end point was 150 °C. The sensitivity analysis shows that the temperature was also affected in production process, the highest value of acetic acid were recorded at the highest temperature.

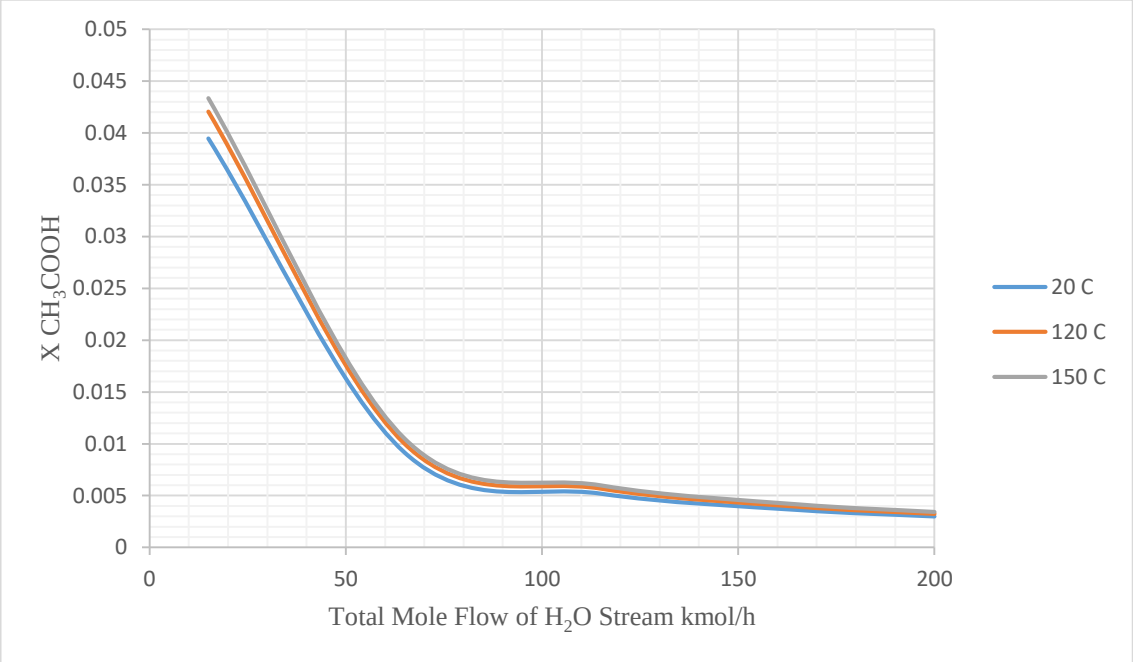

Figure 4.4: The effect of total mole flow and temperature of H_2O on the mole fraction of CH_3COOH.

Figure 4.5 shows the effect of total mole flow with respect to the effect of pressure of H_2O input stream on the mole fraction of CH_3COOH. The start point of mole flow was 15 kmol/hr and the end point was 200 kmol/hr. The increase of the H_2O flow rate decreases the mole fraction of CH_3COOH, which is an inverse relationship. The highest acetic acid mole fraction recorded was at 15 kmol/hr. Moreover, the effect of pressure was analyzed as well. The start point of temperature was 15 bar and end point was 50 bar. The sensitivity analysis shows that there is no effect of pressure in production process, The results recorded were found to be same at different operation pressure. Because the tower that used in production process are better at handling with lower liquid rate, so there is no need for a lot of liquid feed.

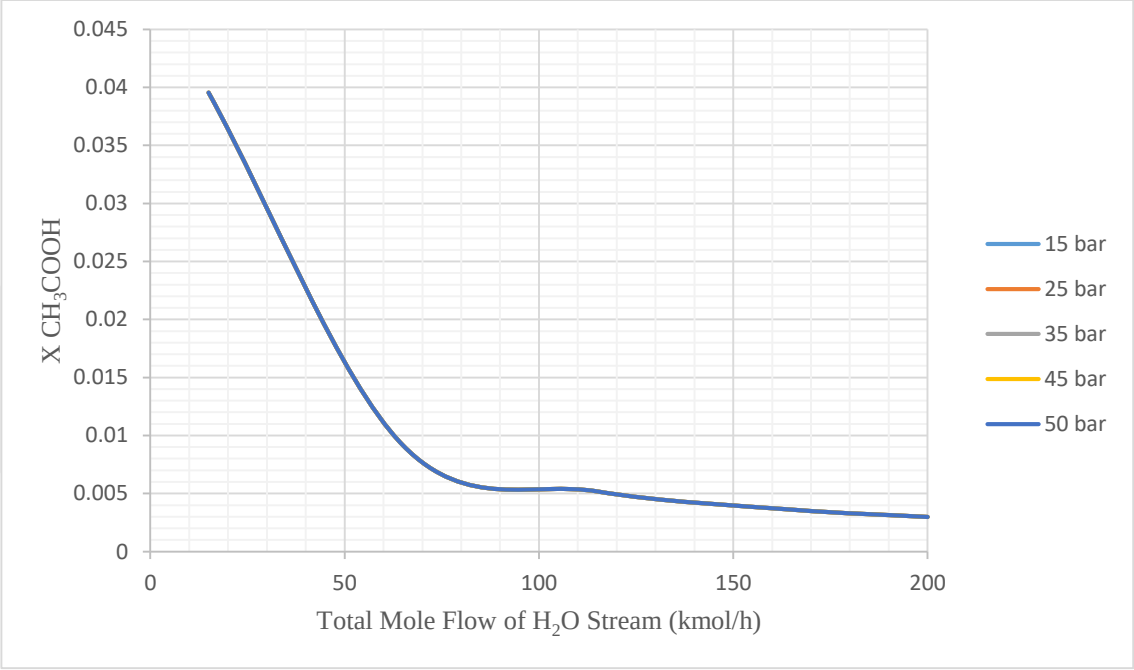

Figure 4.5: The effect of total mole flow and pressure of H_2O on the mole fraction of CH_3COOH.

Figure 4.6 shows the effect of total mole flow with respect to the effect of pressure of H_2O input stream on the mole flow of CH_3COOH. The start point of mole flow was 10 kmol/hr and the end point was 150 kmol/hr. As displayed in the figure, the results of sensitivity analysis shows that there is no effect of the flow rate of H_2O input stream on the mole flow of CH_3COOH. The effect of pressure has been analyzed as well. The sensitivity analysis shows that there is no effect of pressure in production process.

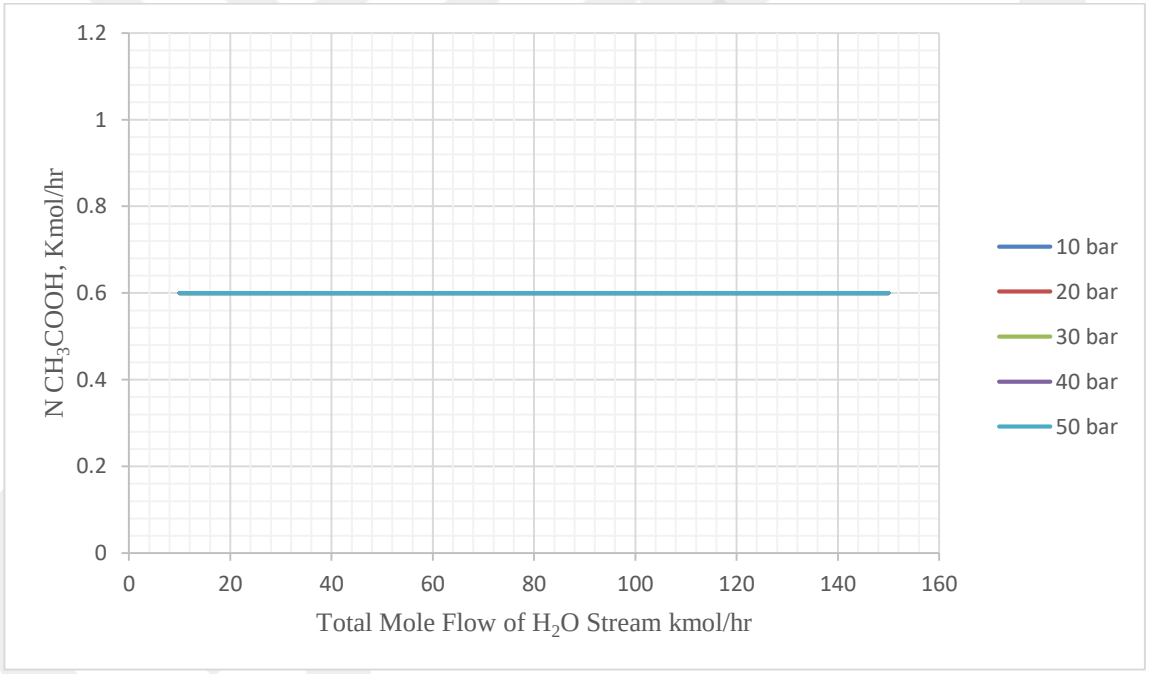

Figure 4.6: The effect of total mole flow and pressure of H_2O on the mole flow of CH_3COOH.

Figure 4.7 shows the results of sensitivity analysis, which indicated that there is no effect of the H_2O mole flow on the mole flow of CH_3COOH. The start point of mole flow was 10 kmol/hr and the end point was 150 kmol/hr as displayed in the figure. The effect of temperature has been analyzed as well. The temperature start point was 20 °C and end point was 150 °C. The sensitivity analysis shows that there is no effect of temperature in production process.

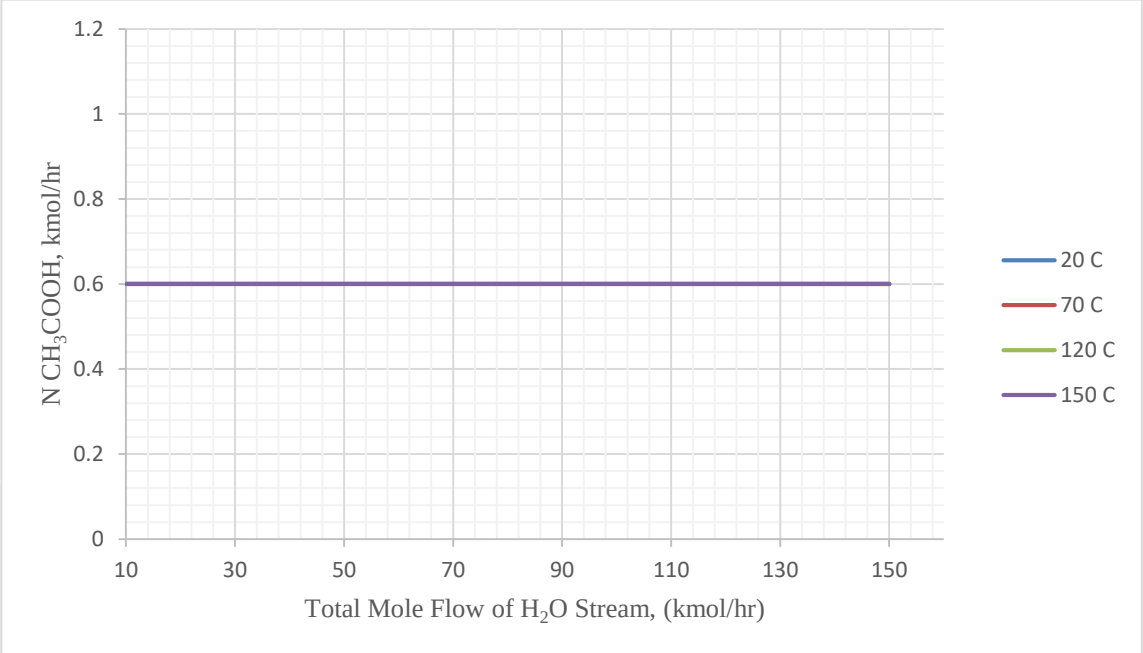

Figure 4.7: The effect of total mole flow and temperature of H_2O stream on the mole flow of CH_3COOH.

2. The Effect of Temperature of H_2O Inlet Stream

Figure 4.8 shows the effect of the temperature with respect to the pressure of H_2O stream on the mole flow of CH_3COOH. The start point of temperature was 5 °C and the end point was 50 °C. As displayed in the figure, the results of sensitivity analysis shows that there is no effect of the total temperature of H_2O input stream on the mole flow of CH_3COOH, which means increasing or decreasing the temperature of H_2O does not change the mole flow of CH_3COOH. The effect of pressure has been analyzed as well. The sensitivity analysis shows that there is no effect of pressure in production process. The start point of pressure was 10 bar and the end point was 20 bar.

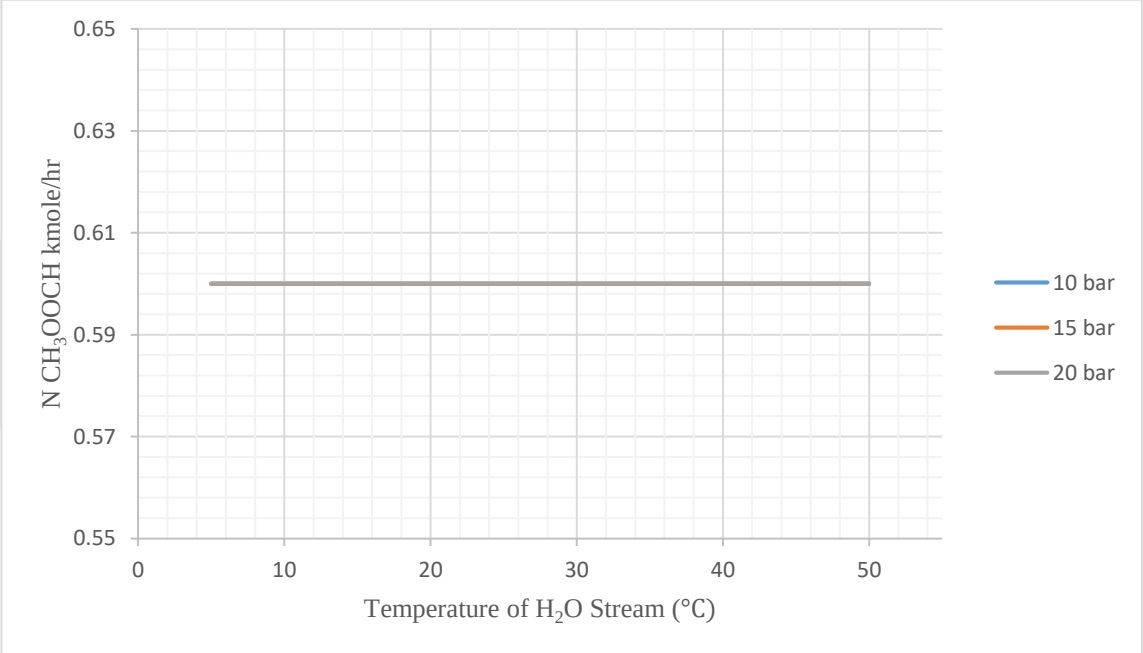

Figure 4.8: The effect of temperature and pressure of H_2O on the mole flow of CH_3COOH.

Figure 4.9 shows the effect of temperature with respect to the pressure of H_2O on the mole fraction of CH_3COOH. The start point of temperature was 10 °C and the end point was 300 °C. The results shows that with increasing temperature of H_2O input stream the mole fraction of CH_3COOH was constant until 210 °C then the CH_3COOH mole fraction started to increase to reach the highest value at end point, which is 300 °C. The highest acetic acid mole fraction recorded was at the end point, because of the heat absorbent process. The higher the temperature produces the higher the purity of acetic acid. In addition, the effect of pressure was analyzed as well. The start point of pressure was 20 bar and end point was 40 bar. The sensitivity analysis shows that the pressure did not affect in production process.

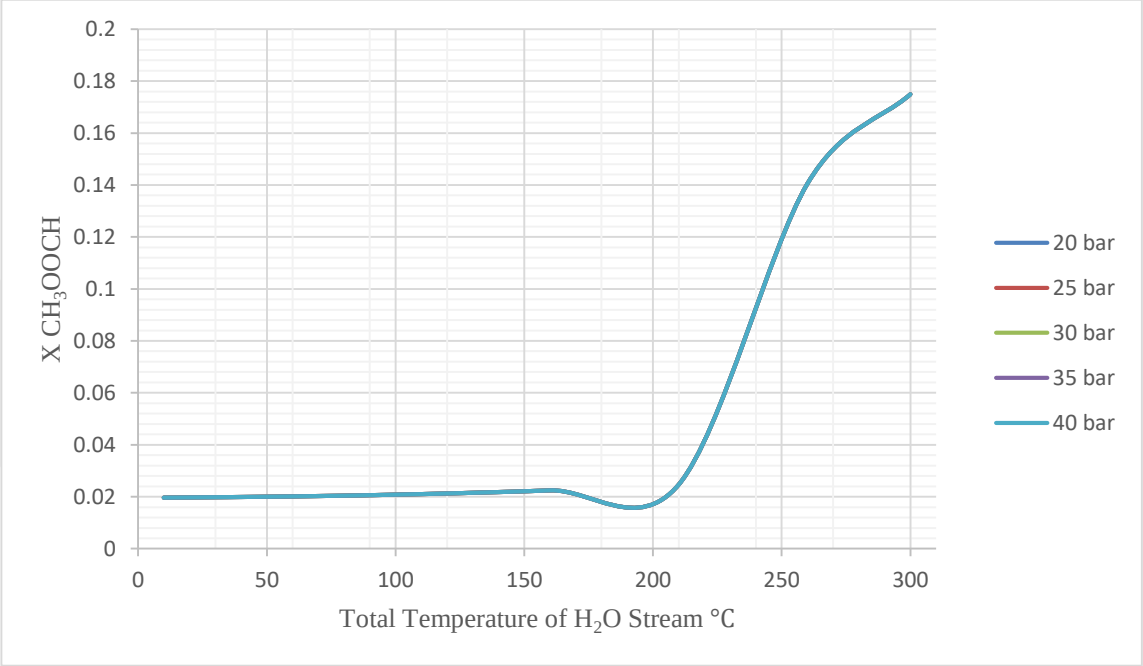

Figure 4.9: The effect of total temperature and pressure of H_2O on the mole fraction of CH_3COOH.

4.2.1.2 The Sensitivity Analysis of CO_2 Stream

1. **The flow rate of CO_2 stream**

CO_2 is the second input stream in RadFrac. Figure 4.10 shows the effect of total mole flow with respect to the temperature of CO_2 stream on the mole fraction of CH_3COOH. The start point of mole flow was 80 kmol/hr and the end point was 1500 kmol/hr. Increase flow rate of CO_2 input stream increases the mole fraction of CH_3COOH as well. The highest acetic acid mole fraction recorded was at the end point of mole flow. Moreover, the effect of temperature was analyzed as well. The start point of temperature was 40 °C and end point was 80 °C. The sensitivity analysis shows that the temperature is also affected in production process, the highest values recorded at the highest temperature, which is 80 °C as shows in figure. Note that the absorption process is controlled in the gas phase and not in the liquid phase, because the gas molecules are converted to liquid phase that means the increase in flow rate increases the absorption rate.

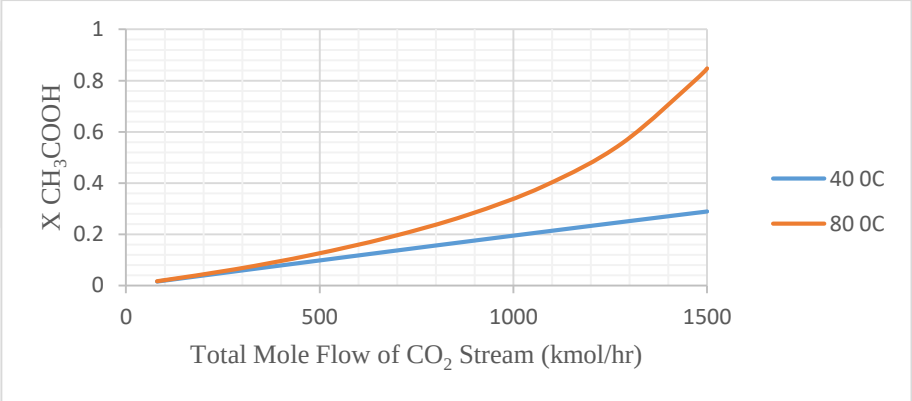

Figure 4.10: The effect of total mole flow and temperature of CO_2 on the mole fraction of CH_3COOH.

Figure 4.11 shows positive relationship between total mole flows of CO_2 stream on the mole fraction of CH_3COOH, with respect to the operation pressure. As variable, the start point of mole flow was 80 kmol/hr and the end point was 1500 kmol/hr. The results indicated that increasing the total mole flows of CO_2 input stream increases the mole fraction of acetic acid as well. On the other hand, the increases in acetic acid mole fraction depended on the operational pressure. The highest acetic acid mole fraction was at the lowest pressure, which is the start point 10 bar, and the end point was 100 bar.

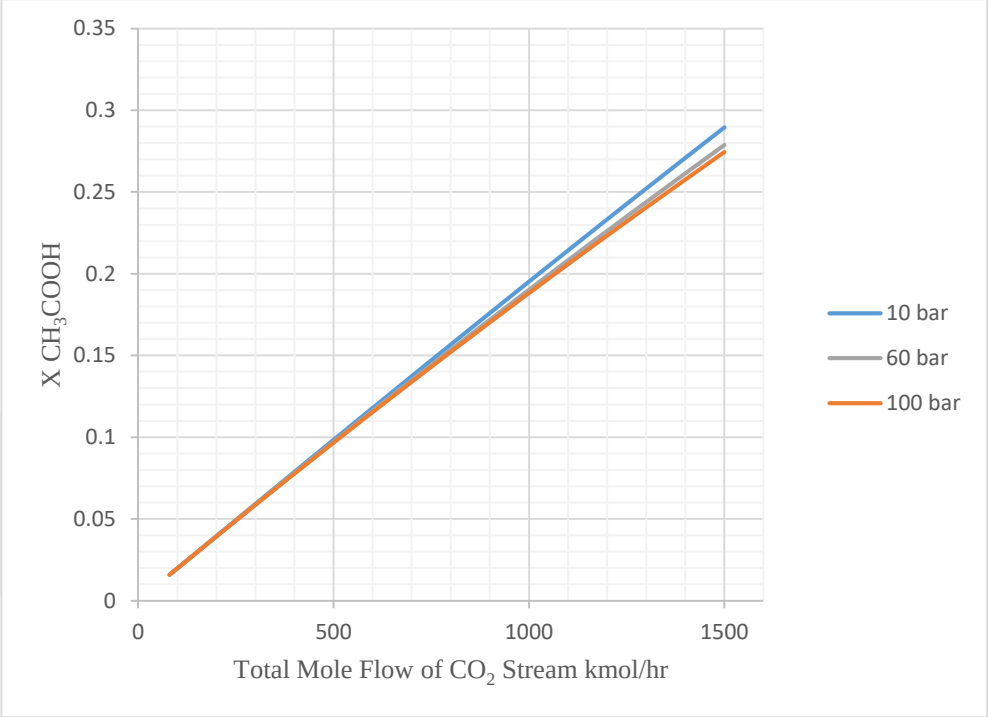

Figure 4.11: The effect of total mole flow and pressure of CO_2 on the mole fraction of CH_3COOH.

The effect of total mole flow with respect to the pressure of CO_2 input stream on the mole flow of CH_3COOH shown in Figure 4.12. In addition, the start point of mole flow was 10 kmol/hr and the end point was 500 kmol/hr. Increase of the CO_2 flow rate increases the mole flow of CH_3COOH. The highest acetic acid mole flow was recorded at 500 kmol/hr. Moreover, the effect of pressure was analyzed. The start point of pressure was 10 bar and end point was 70 bar. The sensitivity analysis shows that there is no effect of pressure in production process, the results recorded are same at different operation pressure.

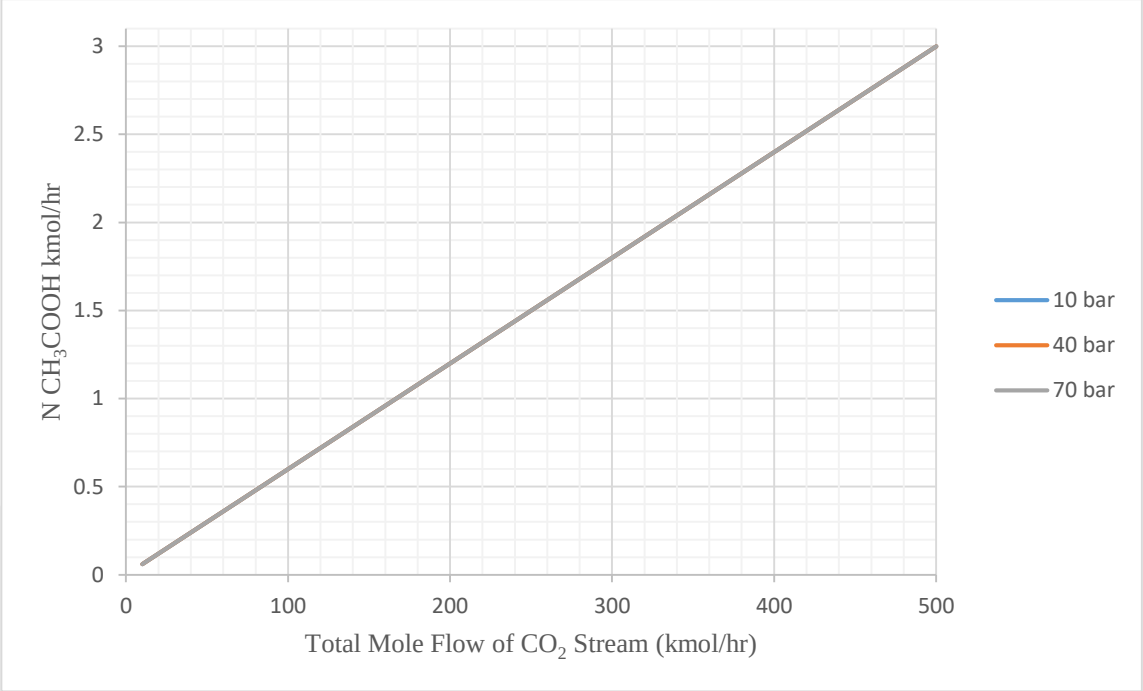

Figure 4.12: The effect of total mole flow and pressure of CO_2 on the mole flow of CH_3COOH.

The effect of total mole flow with respect to the temperature of CO_2 input stream on the mole flow of CH_3COOH shown in Figure 4.13. The start point of mole flow was 10 kmol/hr and the end point was 500 kmol/hr. Figure shows that increase of the CO_2 flow rate increases the mole flow of CH_3COOH as well. The highest acetic acid mole flow

recorded at 500 kmol/hr with respect of operation temperature. The sensitivity analysis of temperature shows the effect of temperature, where the highest results recorded at lowest temperature. The start point of temperature was 30 °C and the end point was 100 °C.

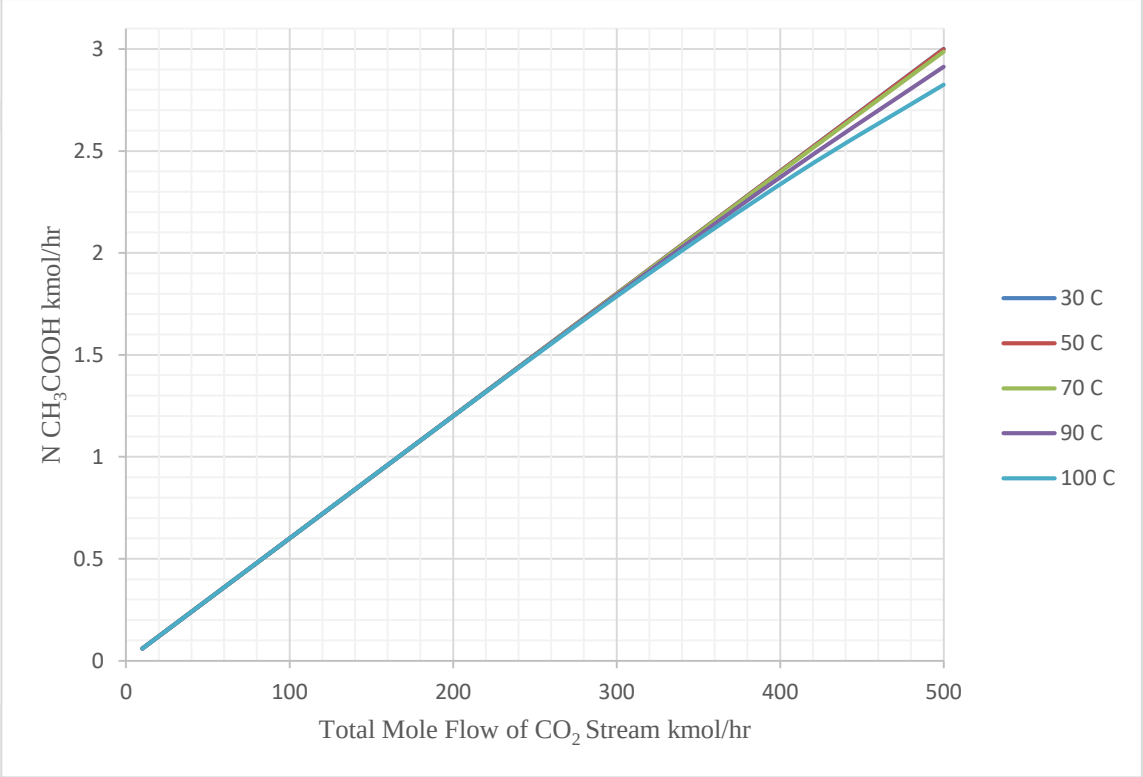

Figure 4.13: The effect of total mole flow and temperature of CO_2 on the mole flow of CH_3COOH.

2. The Effect of Temperature of CO_2 Inlet Stream

Temperature is the second variable of production process parameters. Figure 4.14 shows the effect of total temperature with respect of pressure of CO_2 on the mole flow of CH_3COOH. The start point of temperature was 15 °C and the end point was 400 °C. The results shows that with increasing temperature of CO_2 input stream until 165 °C the mole flow of CH_3COOH was constant at 0.6 kmol/hr then the CH_3COOH mole flow start decreasing to reach the lowest value at the end point, which is 400 °C. The highest acetic acid mole flow recorded was at start point. In addition, the effect of pressure was analyzed as well. The start point of pressure was 15 bar and end point was 30 bar. The sensitivity analysis shows that the pressure did not affect in production process.

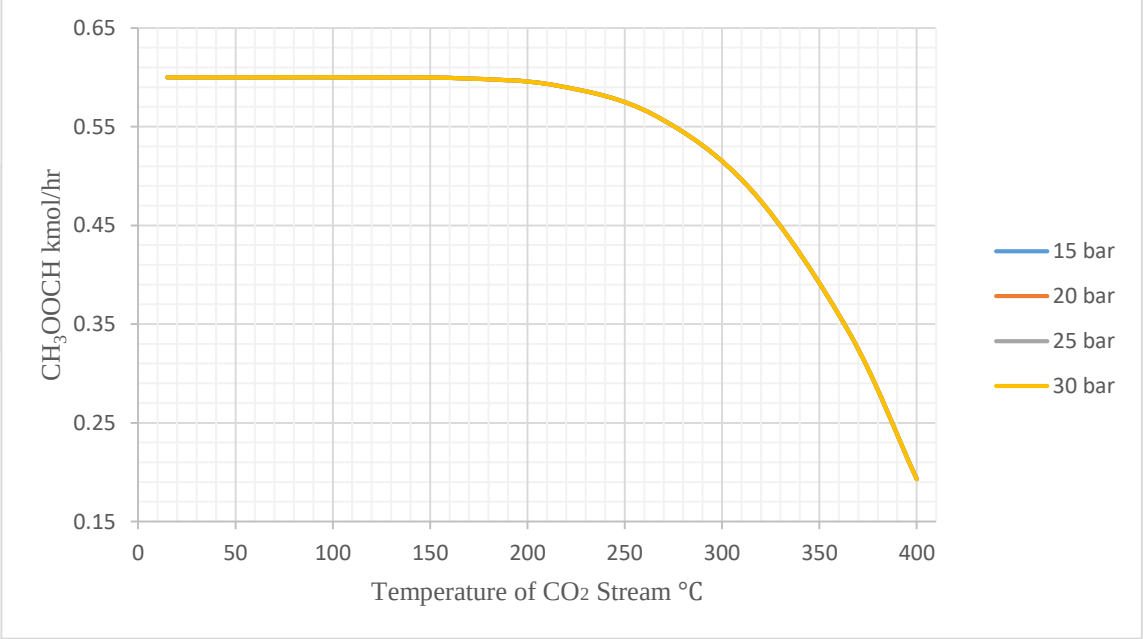

Figure 4.14: The effect of temperature and pressure of CO_2 on the mole flow of CH_3COOH.

Figure 4.15 shows the effect of total temperature with respect to the pressure of CO_2 on the mole fraction of CH_3COOH. The start point of mole flow was 20 °C and the end point was 400 °C. Results shown increase total temperature of CO_2 input stream increases the mole fraction of CH_3COOH. The highest acetic acid mole fraction recorded was at end point. In addition, the effect of pressure was analyzed as well. The start point of pressure was 15 bar and end point was 25 bar. The sensitivity analysis shows that the pressure has no effect on the production process.

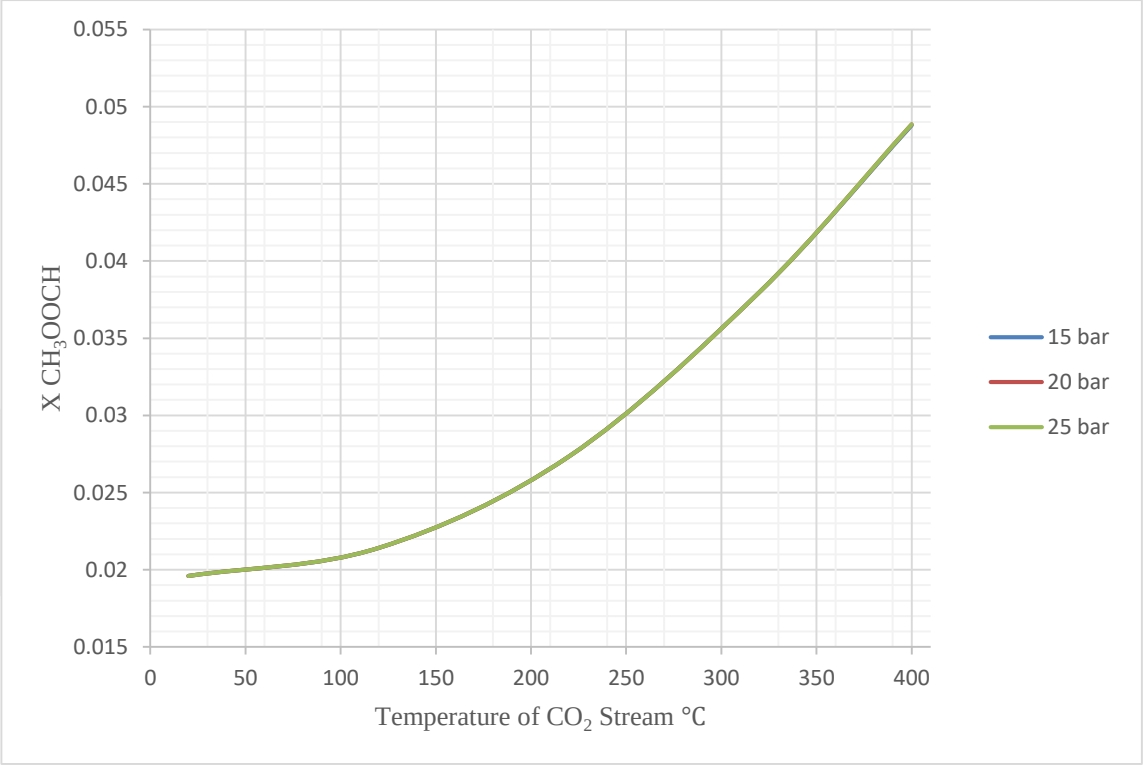

Figure 4.15: The effect of temperature and pressure of CO_2 on the mole fraction of CH_3COOH.

4.2.2 Sensitivity Analysis of CO_2

Figure 4.16 shows the RadFrac inputs for the sensitivity analysis of CO_2. The aim of this sensitivity analysis process is to finding out the effect of various parameters such as the flow rate and temperature throughout RadFrac inputs CO_2 and H_2O on the top stream. All the data of sensitivity analysis are available in Appendices Table 4.18 – 4.27.

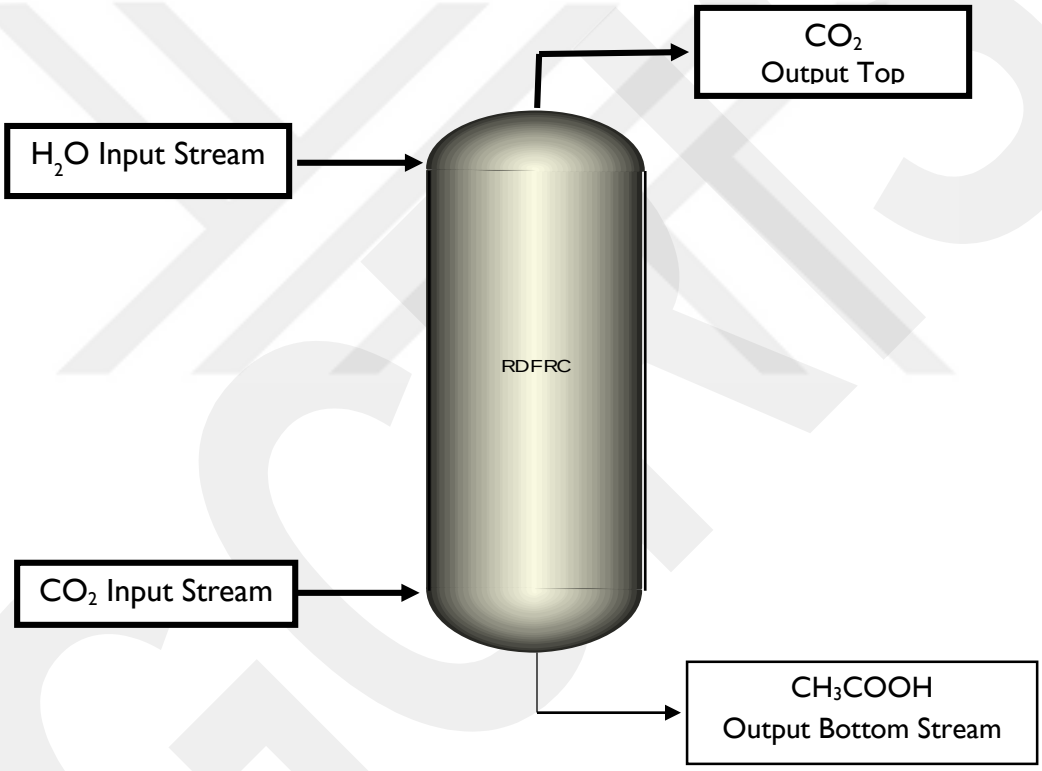

Figure 4.16: The RadFrac inputs in sensitivity analysis of CO_2.

4.2.2.1 The Sensitivity Analysis of the Effect of H_2O Stream

1. **The effect of flow rate of H_2O stream**

Figure 4.17 shows the effect of total mole flow with respect of pressure of H_2O on the mole fraction of CO_2 in top stream. The start point of mole flow was 10 kmol/hr and the end point was 120 kmol/hr. In fact, increase flow rate of H_2O input stream increases the mole fraction of CO_2 until reach 89 kmol/hr then it becomes constant. The highest CO_2 mole fraction recorded was at 110 kmol/hr. the table of data is available in Appendices. Moreover, the effect of pressure was analyzed as well. The start point of pressure was 15 bar and end point was 50 bar. The sensitivity analysis shows that the operation pressure has no affect in production process.

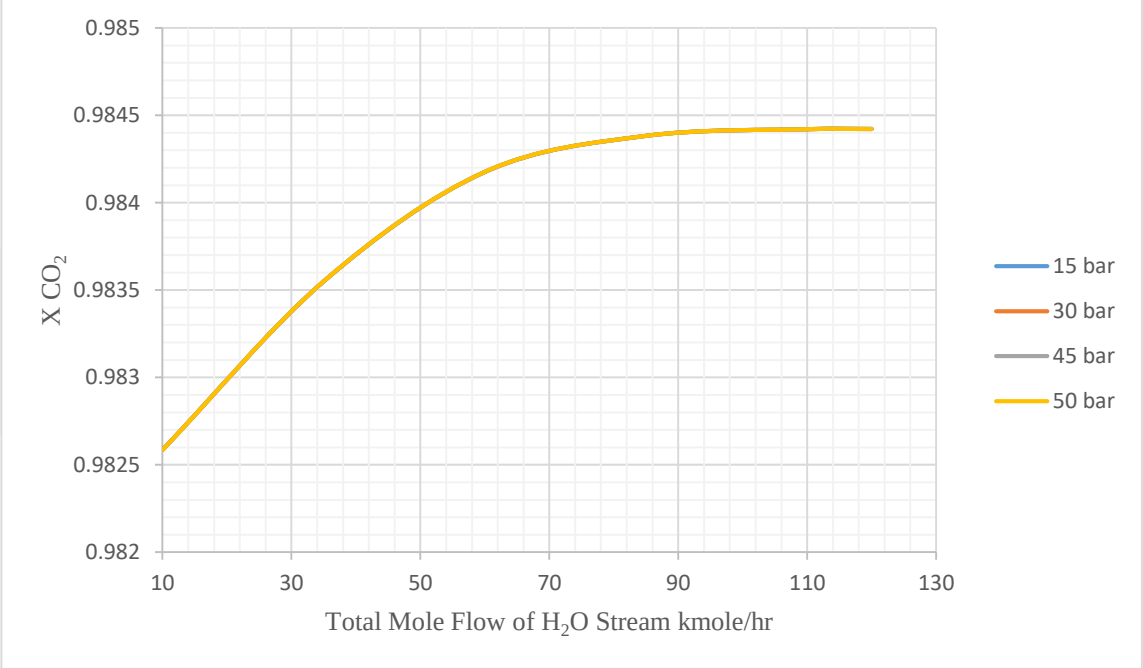

Figure 4.17: The effect of total mole flow and pressure of H_2O on the mole fraction of CO_2.

Figure 4.18 shows the effect of total mole flow with respect to the temperature of H_2O on the mole fraction of CO_2 in top stream. The start point of mole flow was 1 kmol/hr and the end point was 100 kmol/hr. The sensitivity result shows that at lowest temperature 20 °C the relationship between H_2O mole flow and the mole fraction of CO_2 was positive. Increasing the H_2O mole flow increases the mole fraction of CO_2. Then its gradually transformed to inverse relationship with increasing in process temperature until it reaches the lowest value of CO_2 mole fraction and temperature end point 98 °C. The sensitivity analysis shows that the process temperature has strong affect in production process.

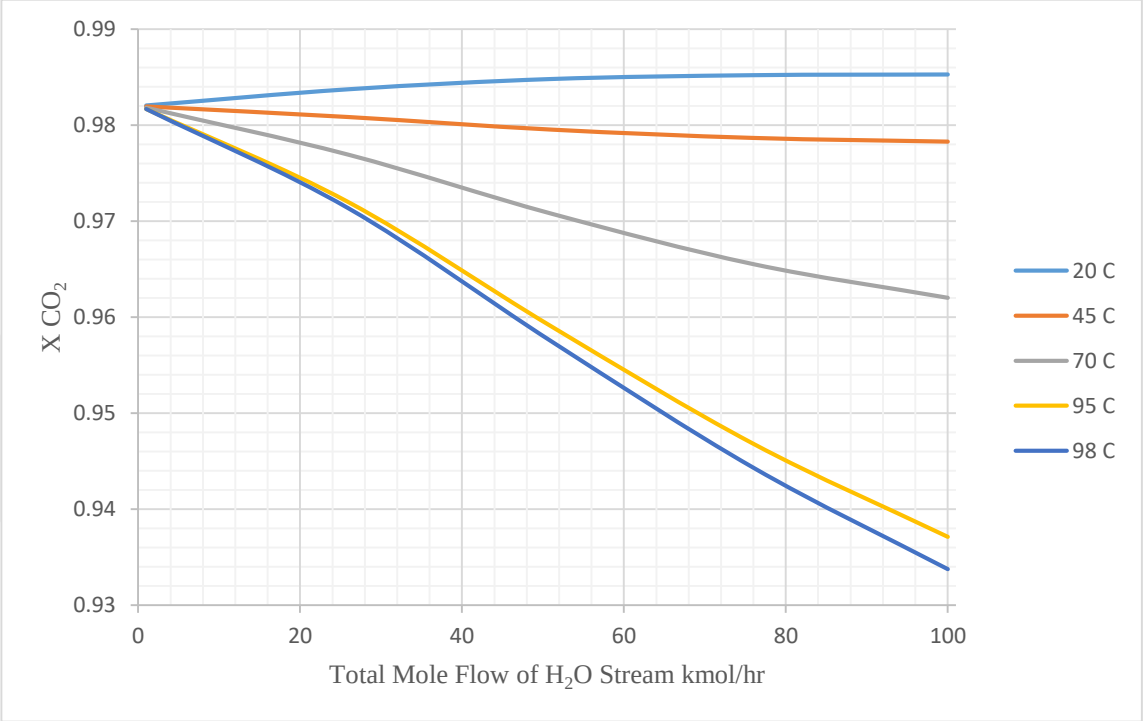

Figure 4.18: The effect of total mole flow and temperature of H_2O on the mole fraction of CO_2.

From Figure 4.19, it is easy to reading an inverse relationship between total mole flow with of H_2O and the mole flow of CO_2 in top stream with respect to the temperature. The start point of mole flow was 1 kmol/he and the end point was 100 kmol/hr. Increasing the H_2O mole flow increases the mole flow of CO_2. Gradually, the mole flow of CO_2 increasing with increasing of temperature until reached the highest value of CO_2 mole flow and the temperature end point 110 °C. The sensitivity analysis shows that the process temperature has strong effect in production process.

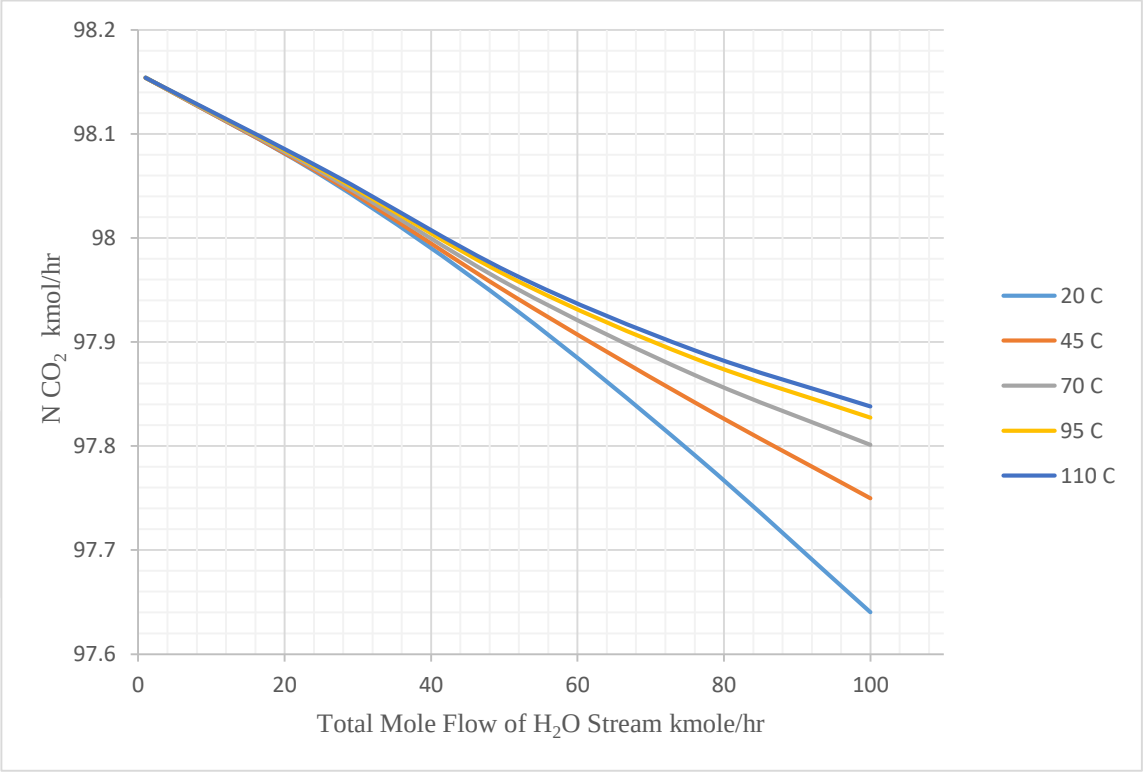

Figure 4.19: The effect of total mol flow and temperature of H_2O on the mol flow of CO_2.

The effect of total mole flow with respect to the pressure of H_2O input stream on the mole flow of CO_2 in top output stream shown in Figure 4.20. The start point of mole flow was 1 kmol/hr and the end point was 100 kmol/hr. Increase of the H_2O flow rate decreases the mole flow of CO_2. The highest CO_2 mole flow recorded at 100 kmol/hr was 97.7 kmol/hr. Moreover, the effect of pressure was analyzed, the start point of pressure was 15 bar and the end point was 50 bar. The sensitivity analysis shows that there is no effect of pressure in production process, the results recorded are same at different process pressure.

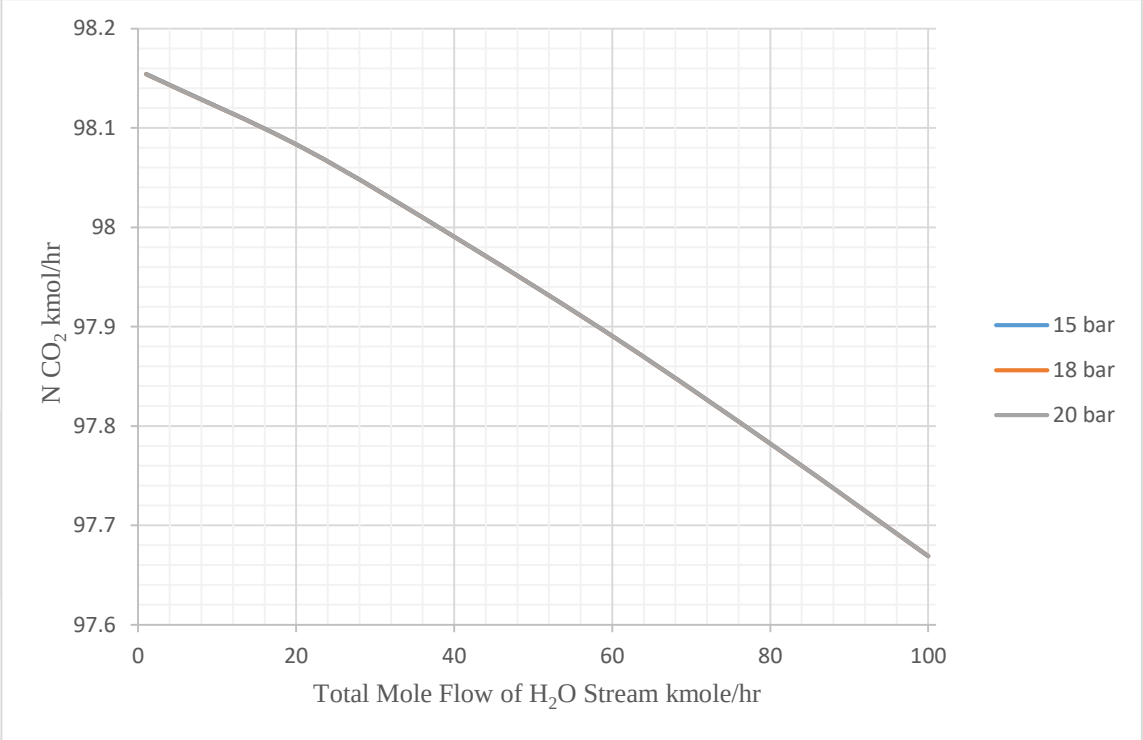

Figure 4.20: The effect of total mole flow and pressure of H_2O on the mole flow of CO_2.

2. The Temperature of H_2O stream

The effect of total temperature and pressure of H_2O input stream on the mole flow and mole fraction of CO_2 shown in Figure 4.2. Increase of the H_2O temperature decreases the mole fraction of CO_2. On other hand, the positive relationship has been indicated between total temperature of H_2O input stream and the mole flow of CO_2, where with increases the temperature of H_2O increases the mole fraction of CO_2 as well. The sensitivity analysis shows that there is no effect of pressure in production process, the results recorded are same at different process pressure in both relationships.

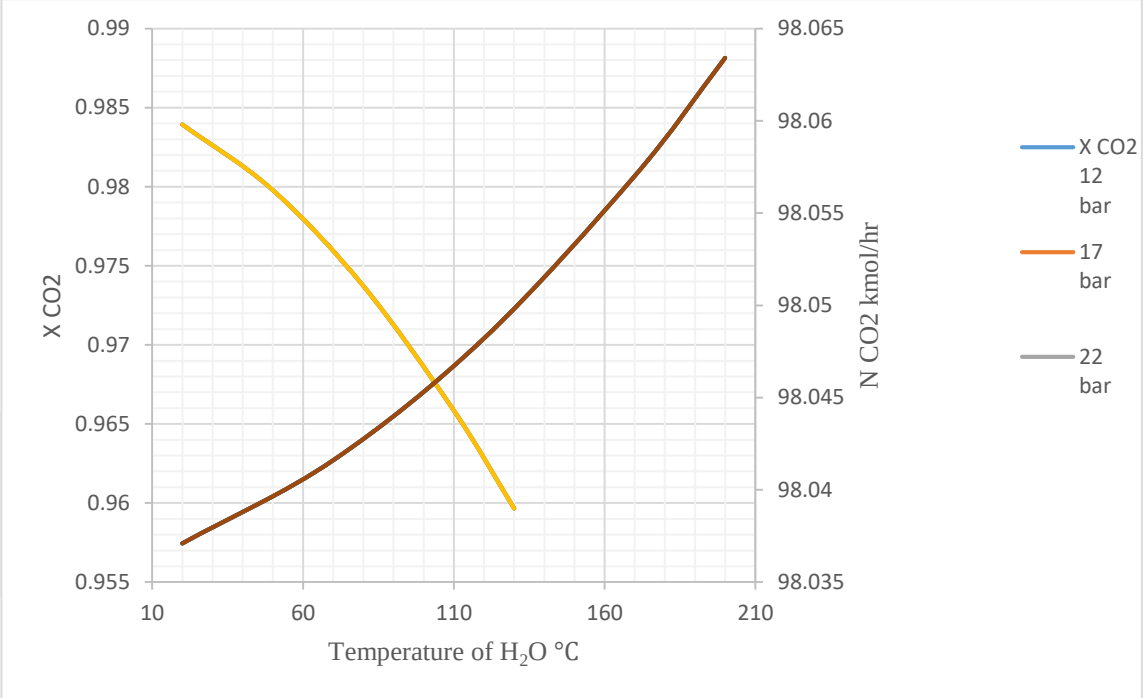

Figure 4.21: The effect of temperature and pressure of H_2O on the mole flow and mole fraction of CO_2.

4.2.2.2 The Sensitivity Analysis of CO_2 Stream

1. **The effect of flow rate of CO_2 stream**

The CO_2 is the second input stream; Figure 4.22 shows the effect of total mole flow with respect of temperature of CO_2 input stream on the mole fraction of CO_2 in top stream. The start point of mole flow was 1 kmol/hr and the end point was 90 kmol/hr. Increasing of the flow rate of CO_2 input stream increases the mole fraction of CO_2 until 30 kmol/hr then the effect of temperature started. Progressively, increasing in process temperature decreases the mole fraction of CO_2 as shown in figure. The optimum CO_2 mole fraction recorded was 0.985 at 10 °C. The start point of temperature was 10 °C and end point was 80 °C.

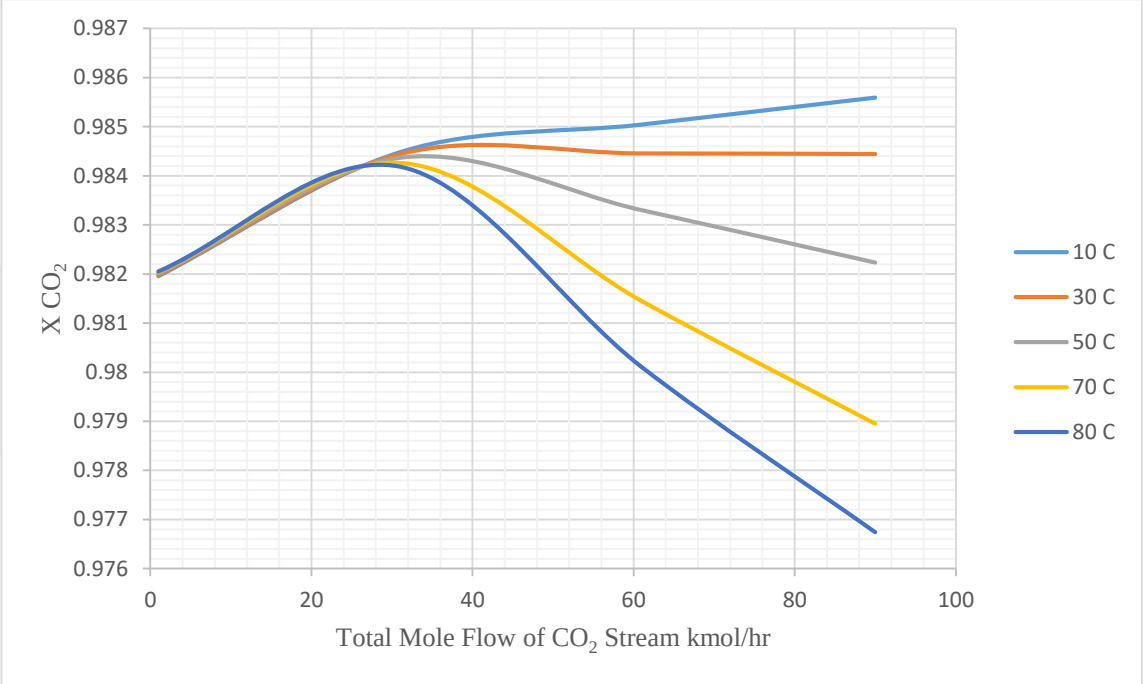

Figure 4.22: The effect of total mole flow and temperature of CO_2 input stream on the mole fraction of CO_2.

Figure 4.23 shows the effect of total mole flow with respect to the process pressure of CO_2 input stream on the mole fraction of CO_2 in top stream. The start point of mole flow was 10 kmol/hr and the end point was 250 kmol/hr. The start point of pressure was 15 bar and end point was 20 bar. The results of sensitivity analysis shows that at start point of total mole flow was the same for all pressures, then progressively the differences was started. The highest mole fraction recorded was 0.99 at 200 bar, as shown in the figure. decreasing the pressure decreasing the mole fraction of CO_2. The sensitivity analysis shows that there is strong effect of pressure in production process.

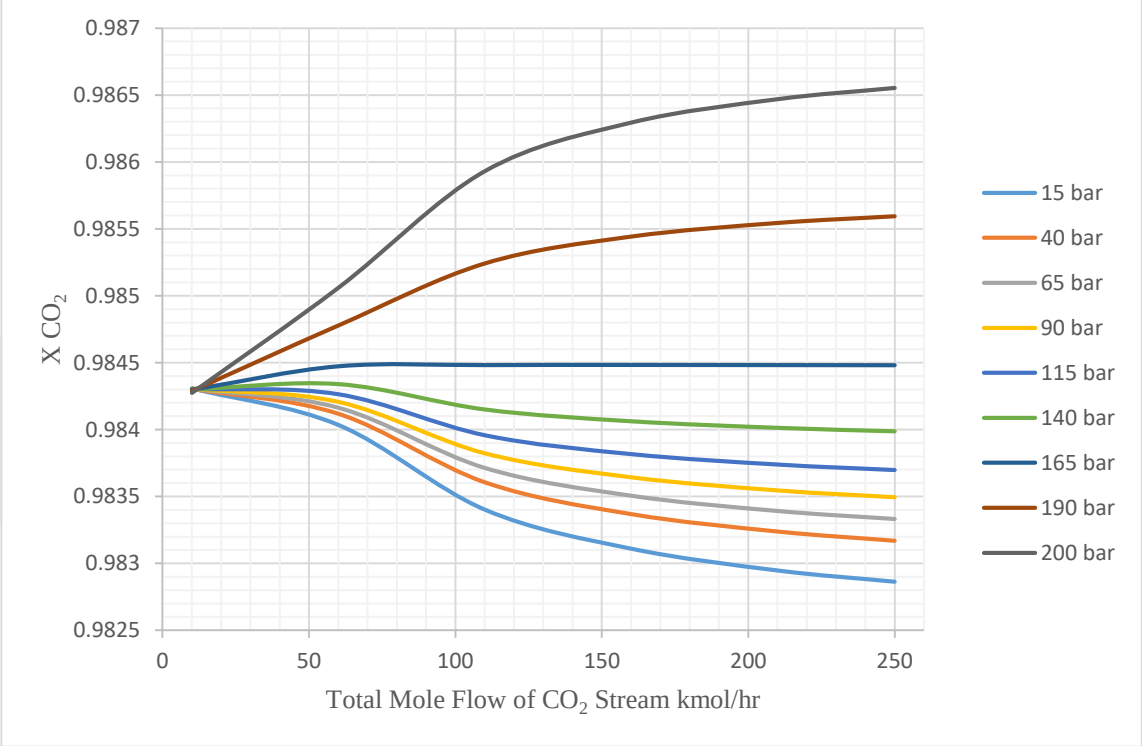

Figure 4.23: The effect of total mole flow and pressure of CO_2 input stream on the mole fraction of CO_2.

Figure 4.24 shows the effect of total mole flow of CO_2 input stream on the mole flow of CO_2 with respect to the temperature. The start point of mole flow was 1 kmol/hr and the end point was 100 kmol/hr, while the start point of temperature was 10 °C and the end point was 50 °C. Increasing total mole flow of CO_2 input stream increases the mole flow of CO_2 as well. The highest CO_2 mole flow recorded was 0.98 mol/hr. In addition, the effect of temperature was analyzed as well. The results of sensitivity analysis shows that the temperature has no effect on the production process.

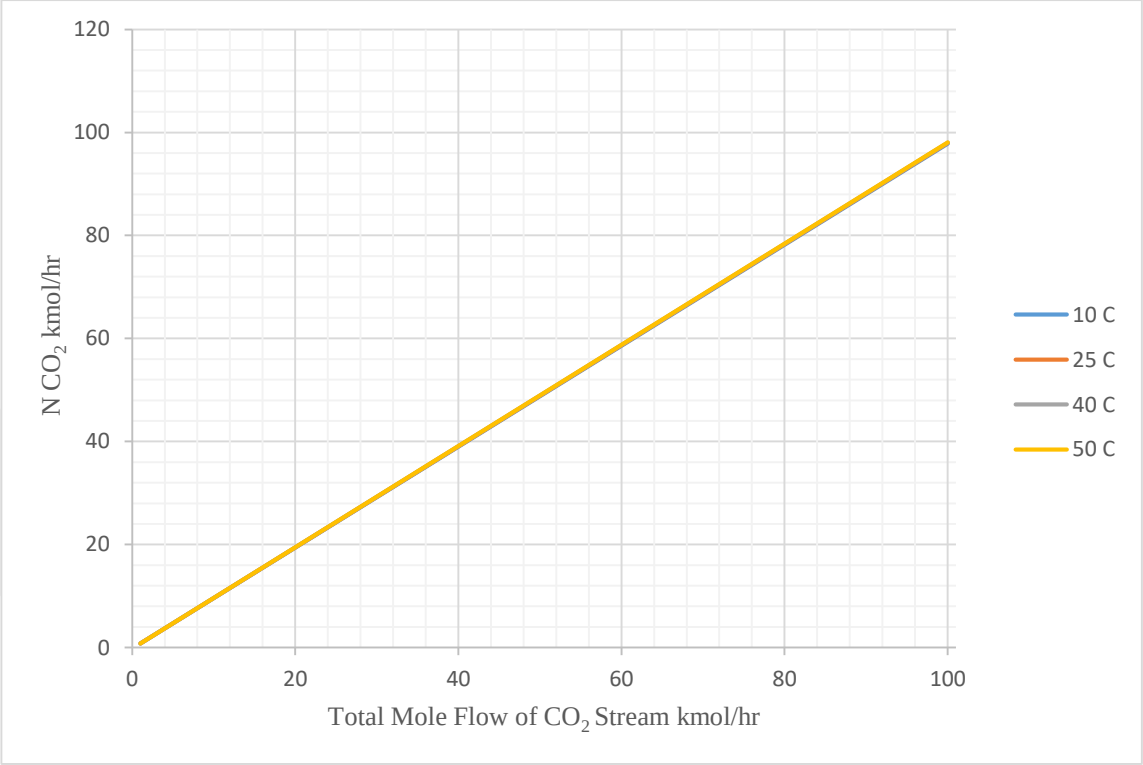

Figure 4.24: The effect of total mole flow and temperature of CO_2 input stream on the mole flow of CO_2.

Like previous figure, Figure 4.25 represents a positive relationship. The effect of total mole flow of CO_2 input stream on the mole flow of CO_2 with respect of pressure has been analyzed. The start point of mole flow was 10 kmol/hr and the end point was 100 kmol/hr, while the start point of pressure was 15 bar and the end point was 25 bar. Increasing total mole flow of CO_2 input stream increases the mole flow of CO_2. The highest CO_2 mole flow recorded was 98 mol/hr. The results of sensitivity analysis shows that the pressure has no effect on the production process.

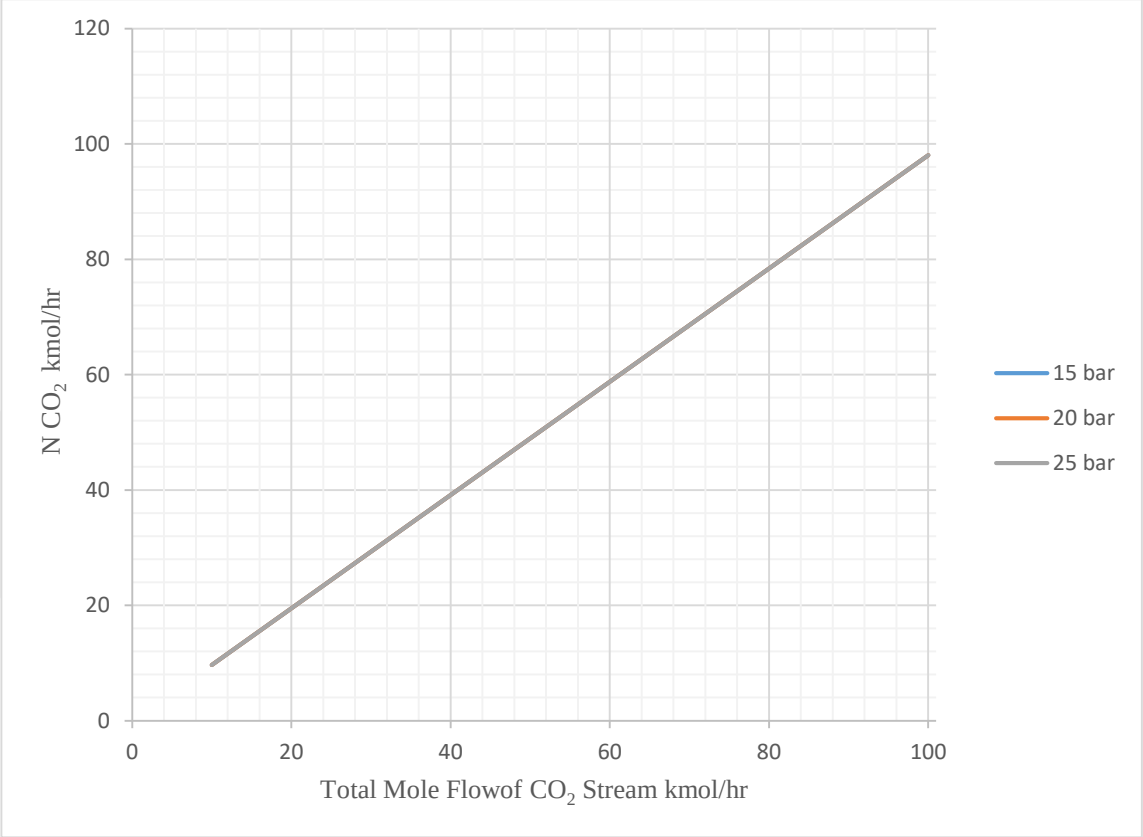

Figure 4.25: The effect of total mole flow and pressure of CO_2 input stream on the mole flow of CO_2.

2. The Effect of Temperature of CO_2 stream

Figure 4.26 shows the effect of the temperature and pressure of CO_2 input stream on the mole flow and mole fraction of CO_2. The inverse relationship has been indicated between the temperature of CO_2 input stream and the mole fraction of CO_2, where with increasing of the CO_2 temperature decreasing the mole fraction of CO_2. The sensitivity analysis shows that there is no effect of pressure in production process. On other hand, Increasing the temperature of CO_2 increases the mole flow of CO_2. The sensitivity analysis shows that there is effect of pressure in production process.

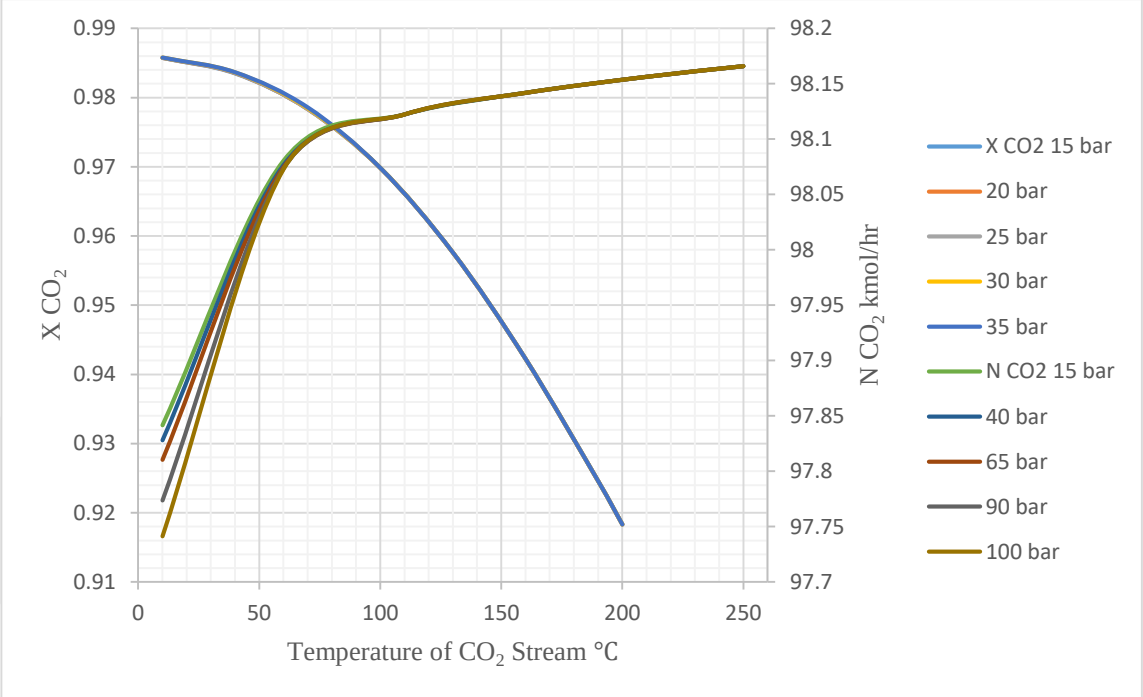

Figure 4.26: The effect of total temperature and pressure of CO_2 input stream on the mole flow and mole fraction of CO_2.

CHAPTER 5

CONCLUSIONS AND RECOMMENDATIONS

This research aims to design and optimize model of acetic acid production by oxidation of ethylene by modeling using Aspen Plus software and also to understand and study the production process of acetic acid, and study the operational variables and their effects on the production. From the simulation, the main conclusions are drawn as following:

1. Acetic acid has been produced as liquid in bottom stream after six stages inside Radfrac. Moreover, the flow rate, temperature and pressure have been controlled and analyzed as sensitivity parameters.
2. The production capacity according to simulation model was 4599 kmol/year, which is about 276177.6 kg/year.
3. The basic product is acetic acid produced as bottom stream with mole flow about 0.6 kmol/hr, at 30.3 °C temperature and 10 bar pressure.
4. The mole fraction of acetic acid produced as bottom stream is about 0.004 at 30.3 °C temperature and 10 bar pressure.
5. According to the simulation results, the optimum mole fraction of acetic acid reached with stages 6 in RadFrac.

6. Increasing flow rate of H_2O input stream decreases the mole fraction of CH_3COOH. The highest acetic acid mole fraction was recorded was at start point or lowest flow rate and highest temperature, while there is no effect of pressure.
7. The results of sensitivity analysis show that there is no effect of the mole flow of H_2O input stream on the mole flow of CH_3COOH, whether with increasing or decreasing the mole flow of H_2O there is no change in the mole flow of CH_3COOH.
8. The results of sensitivity analysis show that there is no effect of the temperature of H_2O input stream on the mole flow of CH_3COOH. With respect to temperature of H_2O input stream the mole fraction of CH_3COOH was constant until 210 °C then the CH_3COOH mole fraction start increasing to reach the highest value at end point, which is 300 °C.
9. The effects that were shown by CO_2 in production process is much more than that shown by H_2O. Positive relationship indicated, with increasing flow rate of CO_2 input stream increases the mole fraction and mole flow of CH_3COOH as well.
10. The results show that increasing temperature of CO_2 input stream the mole flow of CH_3COOH was constant at 0.6 kmol/hr until 165 °C then the CH_3COOH mole flow start decreasing to reach the lowest value at end point, which is 400 °C. Nevertheless, a direct relationship has been noted, with increasing temperature of CO_2 input stream increases the mole fraction of CH_3COOH. The highest acetic acid mole fraction recorded was at end point.

11. The sensitivity analysis shows that with increasing flow rate of H_2O input stream the mole fraction of CO_2 increased as well until reach 110 kmol/hr then it starts to be constant without effect of pressure in production process, but process temperature has strong effect in production process.
12. The sensitivity analysis shows that increasing the H_2O mole flow increases the mole flow of CO_2. In addition, the temperature has strong affect in production process, while there is no effect of pressure.
13. The inverse relationship has been realized between total temperature of H_2O input stream and the mole fraction of CO_2. On other hand, the positive relationship has been indicated between total temperature of H_2O input stream and the mole flow of CO_2.
14. The increasing of the flow rate of CO_2 input stream increases the mole fraction of CO_2, increasing total mole flow of CO_2 input stream increases the mole flow of CO_2 as well, with no effect of temperature and pressure.
15. The inverse relationship has been realized between total temperature of CO_2 input stream and the mole fraction of CO_2. On other hand, the positive relationship has been indicated between total temperature of CO_2 input stream and the mole flow of CO_2.
16. Small amount of CO_2 resulted from conversion of acetic acid and this in turn contribute in decrease of acetic acid production.

REFERENCES

[1] R. E. Jones and D. H. Templeton, "The crystal structure of acetic acid," Acta Crystallographica, vol. 11, pp. 484-487, 1958.

[2] H. M. Awad, R. Diaz, R. A. Malek, N. Z. Othman, R. A. Aziz, and H. A. El Enshasy, "Efficient production process for food grade acetic acid by Acetobacter aceti in shake flask and in bioreactor cultures," Journal of Chemistry, vol. 9, pp. 2275-2286, 2012.

[3] S. Freer, B. Dien, and S. Matsuda, "Production of acetic acid by Dekkera/Brettanomyces yeasts under conditions of constant pH," World Journal of Microbiology and Biotechnology, vol. 19, pp. 101-105, 2003.

[4] R. Riyanto, "Production Of Acetic Acid From Ethanol By Electrolysis (Electrosynthesis)," Jurnal Teknoin, vol. 10, 2005.

[5] C. M. Thomas and G. Süss-Fink, "Ligand effects in the rhodium-catalyzed carbonylation of methanol," Coordination chemistry reviews, vol. 243, pp. 125-142, 2003.

[6] C. Pirola, F. Galli, C. Bianchi, and G. Carvoli, "Heterogeneous distillation of the system water-acetic acid-p-Xylene: study of its fluid phase equilibria, micro-pilot column experimental results and computer simulation," Chemical Engineering Transactions, vol. 32, pp. 1897-1902, 2013.

[7] C. J. Geankoplis, Transport processes and separation process principles, Prentice Hall Professional Technical Reference, 2003.

[8] K. i. Sano, H. Uchida, and S. Wakabayashi, "A new process for acetic acid production by direct oxidation of ethylene," Catalysis Surveys from Asia, vol. 3, pp. 55-60, 1999.

[9] F. Gallia, D. P. , S. C. , C. P. , F. , Manentib, et al., "Simulation of the Water-Acetic Acid Separation via Distillation Using Different Entrainers: an Economic Comparison," Chemical Engineering Transactions, vol. VOL. 57, 2017 2017.

[10] M. Schaechter, Encyclopedia of microbiology: Academic Press, 2009.

[11] Y. S. Park, H. Ohtake, K. Toda, M. Fukaya, H. Okumura, and Y. Kawamura, "Acetic acid production using a fermentor equipped with a hollow fiber filter module," Biotechnology and bioengineering, vol. 33, pp. 918-923, 1989.

[12] N. Yoneda, S. Kusano, M. Yasui, P. Pujado, and S. Wilcher, "Recent advances in processes and catalysts for the production of acetic acid," Applied Catalysis A: General, vol. 221, pp. 253-265, 2001.

[13] S. Xu, L. Wang, W. Chu, and W. Yang, "Influence of Pd precursors on the catalytic performance of Pd–H 4 SiW 12 O 40/SiO 2 in the direct oxidation of ethylene to acetic acid," Journal of Molecular Catalysis A: Chemical, vol. 310, pp. 138-143, 2009.

[14] H. Jones Jone, "The Cativa Process For The Manufacture Plant Of Acetic Acid Iridium Catalyst Improves Productivity In An Established Industrial Process," ed: BP Chemicals Ltd., Hull Research &Technology Centre, Salt End, Hull HU12 8DS, UK.

[15] F. Roth, "The Production of Acetic Acid Rhodium Catalysed Carbonylation Of Methanol."Platinum Metals Rev., 19 (1), 1975.

[16] W. Chu, Y. Ooka, Y. Kamiya, and T. Okuhara, "Reaction path for oxidation of ethylene to acetic acid over Pd/WO 3–ZrO 2 in the presence of water," Catalysis letters, vol. 101, pp. 225-228, 2005.

[17] J. J. McKetta Jr, Encyclopedia of chemical processing and design: CRC press, 1997.

[18] J. T. Yeh, H. W. Pennline, and K. P. Resnik, "Study of CO2 absorption and desorption in a packed column," Energy & fuels, vol. 15, pp. 274-278, 2001.

[19] E.Y. Kenig, L. Kucka, A. Gorak, "Rigorous modeling of reactive absorption processes," Chemical Engineering & Technology, 26 (6), pp. 631-646, 2003.

[20] Ö. Yildirim, A.A.Kiss, N. Hüser, K. Lessmann, E. Y. Kenid, "Reactive absorption in chemical process industry: A review on current activities" The Chemical Engineering Journal, 213, pp. 371-391, 2012.

[21] J. Fair, D. Steinmeyer, W. Penney, and B. Crocker, "Gas absorption and gas-liquid system design, chapter 14," Perry's Chemical Engineering Handbook, 2001.

[22] J. D. Seader, E. J. Henley, and D. K. Roper, "Separation process principles," 1998.

[23] W. Ho and K. Sirkar, Membrane handbook: Springer Science & Business Media, 2012.

[24] D. Mackay and W. Y. Shiu, "A critical review of Henry's law constants for chemicals of environmental interest," Journal of physical and chemical reference data, vol. 10, pp. 1175-1199, 1981.

[25] R. Sander, "Compilation of Henry's law constants for inorganic and organic species of potential importance in environmental chemistry," ed: Max-Planck Institute of Chemistry, Air Chemistry Department Mainz, Germany, 1999.

[26] D. Mackay, W. Y. Shiu, and R. P. Sutherland, "Determination of air-water Henry's law constants for hydrophobic pollutants," Environmental Science & Technology, vol. 13, pp. 333-337, 1979.

[27] J. Sotelo, F. Beltran, F. Benitez, and J. Beltran-Heredia, "Henry's law constant for the ozone-water system," Water Research, vol. 23, pp. 1239-1246, 1989.

[28] C. Somers, A. Mortazavi, Y. Hwang, R. Radermacher, P. Rodgers, and S. Al-Hashimi, "Modeling water/lithium bromide absorption chillers in ASPEN Plus," Applied Energy, vol. 88, pp. 4197-4205, 2011.

[29] L. E. Øi, "Aspen HYSYS simulation of CO2 removal by amine absorption from a gas based power plant," in The 48th Scandinavian Conference on Simulation and Modeling (SIMS 2007); 30-31 October; 2007; Göteborg (Särö), 2007, pp. 73-81.

[30] L. ErikØi, "Comparison of Aspen HYSYS and Aspen Plus simulation of CO2 absorption into MEA from atmospheric gas," Energy Procedia, vol. 23, pp. 360-369, 2012.

[31] M. H. Murad Chowdhury, X. Feng, P. Douglas, and E. Croiset, "A new numerical approach for a detailed multicomponent gas separation membrane model and AspenPlus simulation," Chemical engineering & technology, vol. 28, pp. 773-782, 2005.

[32] S. Venkataraman, W. K. Chan, and J. Boston, "Reactive distillation using ASPEN PLUS," Chemical Engineering Progress, vol. 86, pp. 45-54, 1990.

APPENDICES

The Data of Sensitivity Analysis of CH_3COOH

Table 4.5: Liquid mole fractions of acetic acid at each stage.

Stage	Mole fraction CH_3COOH
1	1.68E-14
2	3.36E-12
3	6.64E-10
4	1.29E-7
5	2.37E-5
6	3.97E-3

Table 4.6: The effect of total mole flow and temperature of H_2O on the mole fraction of CH_3COOH.

Temperature	15 kmol/hr	65 kmol/hr	115 kmol/hr	165 kmol/hr	200 kmol/hr
20 C	0.0394536	0.00913792	0.00517252	0.00360732	0.00297677
120 C	0.0420438	0.00998737	0.00565822	0.00392504	0.00322455
150 C	0.0433374	0.0104956	0.00597945	0.00415716	0.00341779

Table 4.7: The effect of total mole flow and pressure of H_2O on the mole fraction of CH_3COOH.

Pressure	15 kmol/hr	65 kmol/hr	115 kmol/hr	165 kmol/hr	200 kmol/hr
15 bar	0.0395366	0.00915064	0.00517808	0.00361085	0.00297957
25 bar	0.0395366	0.00915064	0.00517807	0.00361085	0.00297958
35 bar	0.0395366	0.00915064	0.00517807	0.00361085	0.00297958
45 bar	0.0395366	0.00915063	0.00517807	0.00361085	0.00297958
50 bar	0.0395366	0.00915063	0.00517807	0.00361085	0.00297958

Table 4.8: The effect of total mole flow and pressure of H_2O on the mole flow of CH_3COOH.

Pressure	10 kmol/hr	30 kmol/hr	50 kmol/hr	70 kmol/hr	90 kmol/hr	110 kmol/hr	130 kmol/hr	150 kmol/hr
10 bar	0.599999	0.6	0.6	0.6	0.6	0.6	0.6	0.6
20 bar	0.599999	0.6	0.6	0.6	0.6	0.6	0.6	0.6
30 bar	0.599999	0.6	0.6	0.6	0.6	0.6	0.6	0.6
40 bar	0.599999	0.6	0.6	0.6	0.6	0.6	0.6	0.6
50 bar	0.599999	0.6	0.6	0.6	0.6	0.6	0.6	0.6

Table 4.9: The effect of total mole flow and temperature of H_2O on the mole flow of CH_3COOH.

Temperature	10 kmol/hr	40 kmol/hr	70 kmol/hr	100 kmol/hr	130 kmol/hr	150 kmol/hr
20 C	0.599999	0.6	0.6	0.6	0.6	0.6
70 C	0.599998	0.6	0.6	0.6	0.6	0.6
120 C	0.599997	0.6	0.6	0.6	0.6	0.6
150 C	0.599996	0.6	0.6	0.6	0.6	0.6

Table 4.10: The effect of total temperature and pressure of H_2O on the mole flow of CH_3COOH.

Pressure	5 ^{0}C	25 ^{0}C	45 ^{0}C	50 ^{0}C
10 bar	0.6	0.6	0.6	0.6
15 bar	0.6	0.6	0.6	0.6
20 bar	0.6	0.6	0.6	0.6

Table 4.11: The effect of total temperature and pressure of H_2O on the mole fraction of CH_3COOH.

Pressure	10 ^{0}C	60 ^{0}C	110 ^{0}C	160 ^{0}C	210 ^{0}C	260 ^{0}C	300 ^{0}C
20 bar	0.0196969	0.0201671	0.0210627	0.0224897	0.024693	0.140525	0.174973
25 bar	0.019697	0.020167	0.0210627	0.0224897	0.024693	0.140526	0.174974
30 bar	0.019697	0.020167	0.0210627	0.0224897	0.024693	0.140526	0.174974
35 bar	0.019697	0.020167	0.0210627	0.0224897	0.0246929	0.140526	0.174974
40 bar	0.019697	0.020167	0.0210627	0.0224897	0.024693	0.140526	0.174974

Table 4.12: The effect of total mole flow and temperature of CO_2 on the mole fraction of CH_3COOH.

Temperature	80 kmol/hr	280 kmol/hr	480 kmol/hr	680 kmol/hr	880 kmol/hr	1080 kmol/hr	1280 kmol/hr	1480 kmol/hr	1500 kmol/hr
40 ^{0}C	0.0158449	0.0552868	0.0945052	0.133475	0.172159	0.210481	0.24839	0.285814	0.28953
80 ^{0}C	0.0161367	0.06246	0.119228	0.188257	0.274389	0.388795	0.55457	0.816078	0.84739

Table 4.13: The effect of total mole flow and pressure of CO2 on the mole fraction of CH3COOH.

Pressure	80 kmol/hr	280 kmol/hr	480 kmol/hr	680 kmol/hr	880 kmol/hr	1080 kmol/hr	1280 kmol/hr	1480 kmol/hr	1500 kmol/hr
10 bar	0.0158449	0.0552874	0.0945044	0.133475	0.172155	0.210478	0.248388	0.285813	0.289527
60 bar	0.0158266	0.0549257	0.0933719	0.131161	0.168281	0.204706	0.240409	0.275366	0.278816
100 bar	0.0158185	0.0547714	0.0928946	0.130197	0.166675	0.202325	0.237135	0.271092	0.27444

Table 4.14: The effect of total mole flow and pressure of CO_2 on the mole flow of CH_3COOH.

Pressure	10 kmol/hr	110 kmol/hr	210 kmol/hr	310 kmol/hr	410 kmol/hr	500 kmol/hr
10 bar	0.06	0.66	1.26	1.86	2.45997	2.99991
40 bar	0.06	0.66	1.26	1.86	2.45999	2.99995
70 bar	0.06	0.66	1.26	1.86	2.45999	2.99996

Table 4.15: The effect of total mole flow and temperature of CO_2 on the mole flow of CH_3COOH.

Temperature	10 kmol/hr	110 kmol/hr	210 kmol/hr	310 kmol/hr	410 kmol/hr	500 kmol/hr
30 C	0.06	0.66	1.26	1.86	2.46	2.99999
50 C	0.06	0.66	1.26	1.85997	2.45979	2.99927
70 C	0.06	0.659999	1.25994	1.85926	2.45588	2.98726
90 C	0.06	0.659994	1.2594	1.85305	2.42713	2.91337
100 C	0.06	0.659983	1.25842	1.84323	2.38809	2.82477

Table 4.16: The effect of total temperature and pressure of CO_2 on the mole flow of CH_3COOH.

Pressure	15 ^{0}C	65 ^{0}C	115 ^{0}C	165 ^{0}C	215 ^{0}C	265 ^{0}C	315 ^{0}C	365 ^{0}C	400 ^{0}C
15 bar	0.6	0.6	0.599967	0.599075	0.591704	0.561876	0.485658	0.342404	0.192822
20 bar	0.6	0.6	0.599967	0.599075	0.591706	0.561879	0.485952	0.342455	0.192938
25 bar	0.6	0.6	0.599967	0.599075	0.591706	0.561879	0.485953	0.342454	0.192937
30 bar	0.6	0.6	0.599967	0.599075	0.591706	0.561879	0.485953	0.342453	0.192938

Table 4.17: The effect of total temperature and pressure of CO_2 on the mole fraction of CH_3COOH.

Pressure	20 ^{0}C	120 ^{0}C	220 ^{0}C	320 ^{0}C	400 ^{0}C
15 bar	0.0196101	0.0214244	0.0273515	0.0379821	0.0487759
20 bar	0.0196075	0.0214244	0.0273518	0.0379835	0.0488477
25 bar	0.0196054	0.0214244	0.0273518	0.0379835	0.0488472

The Data of sensitivity Analysis of CO_2

Table 4.18: The effect of total mole flow and pressure of H_2O on the mole fraction of CO_2.

Pressure	10 kmol/hr	35 kmol/hr	60 kmol/hr	85 kmol/hr	110 kmol/hr	120 kmol/hr
15 bar	0.982585	0.983549	0.984176	0.984383	0.984421	0.984423
30 bar	0.982585	0.98355	0.984176	0.984383	0.984421	0.984422
45 bar	0.982585	0.98355	0.984177	0.984383	0.984421	0.984422
50 bar	0.982585	0.98355	0.984177	0.984383	0.984421	0.984422

Table 4.19: The effect of total mole flow and temperature of H_2O on the mole fraction of CO_2.

Temperature	1 kmol/hr	26 kmol/hr	51 kmol/hr	76 kmol/hr	100 kmol/hr
20 C	0.98205	0.983727	0.984785	0.985181	0.985254
45 C	0.981931	0.980827	0.979525	0.978659	0.978274
70 C	0.981808	0.976909	0.970785	0.965513	0.96201
95 C	0.981679	0.971968	0.959059	0.946811	0.937128
98 C	0.981662	0.971308	0.957487	0.944299	0.93374

Table 4.20: The effect of total mole flow and temperature of H_2O on the mole flow of CO_2.

Temperature	1 kmol/hr	26 kmol/hr	51 kmol/hr	76 kmol/hr	100 kmol/hr
20 C	98.1542	98.0558	97.9339	97.7912	97.6402
45 C	98.1541	98.0574	97.9453	97.8421	97.7499
70 C	98.1541	98.0594	97.9539	97.8682	97.8011
95 C	98.1541	98.0618	97.9616	97.8843	97.8274
110 C	98.1541	98.0634	97.9661	97.8921	97.8382

Table 4.21: The effect of total mole flow and pressure of H_2O on the mole flow of CO_2.

Pressure	1 kmol/hr	21 kmol/hr	41 kmol/hr	61 kmol/hr	81 kmol/hr	100 kmol/hr
15 bar	98.1542	98.0792	97.9855	97.8853	97.7767	97.6689
18 bar	98.1541	98.0792	97.9855	97.8853	97.7766	97.6689
20 bar	98.1541	98.0792	97.9855	97.8853	97.7766	97.6689

Table 4.22: The effect of total temperature and pressure of H_2O on the mole flow and mole fraction of CO_2.

X CO2	20 ^{0}C	50 ^{0}C	80 ^{0}C	110 ^{0}C	130 ^{0}C
12 bar	0.983936	0.979785	0.973726	0.965851	0.959657
17 bar	0.983936	0.979785	0.973727	0.965848	0.959656
22 bar	0.983936	0.979786	0.973726	0.965848	0.959656
25 bar	0.983935	0.979786	0.973726	0.965848	0.959656

N CO2	20 ^{0}C	70 ^{0}C	120 ^{0}C	170 ^{0}C	200 ^{0}C
16 bar	98.0371	98.0416	98.0482	98.057	98.0634
20 bar	98.0371	98.0416	98.0482	98.057	98.0634
24 bar	98.0371	98.0416	98.0482	98.057	98.0634
25 bar	98.0371	98.0416	98.0482	98.057	98.0634

Table 4.23: The effect of total mole flow and temperature of CO_2 input stream on the mole fraction of CO_2.

Temperature	1 kmol/hr	31 kmol/hr	61 kmol/hr	90 kmol/hr
10 C	0.981953	0.98448	0.985044	0.985593
30 C	0.981981	0.984442	0.984454	0.984443
50 C	0.982011	0.984369	0.9833	0.982231
70 C	0.982038	0.984262	0.981451	0.978953
80 C	0.982052	0.984185	0.980107	0.976743

Table 4.24: The effect of total mole flow and pressure of CO_2 input stream on the mole fraction of CO_2.

Pressure	10 kmol/hr	60 kmol/hr	110 kmol/hr	160 kmol/hr	210 kmol/hr	250 kmol/hr
15 bar	0.984308	0.984035	0.983402	0.98311	0.982947	0.982863
40 bar	0.984306	0.984119	0.983607	0.983369	0.983239	0.98317
65 bar	0.984306	0.984164	0.983714	0.983506	0.983392	0.983332
90 bar	0.984305	0.984207	0.983823	0.983644	0.983546	0.983495
115 bar	0.984304	0.984263	0.983957	0.983816	0.983738	0.983697
140 bar	0.984302	0.98434	0.984151	0.984063	0.984014	0.983988
165 bar	0.984298	0.984472	0.984481	0.984482	0.984481	0.98448
190 bar	0.984288	0.984778	0.985242	0.985443	0.985545	0.985595
200 bar	0.984275	0.98506	0.985931	0.986294	0.986469	0.986553

Table 4.25: The effect of total mole flow and temperature of CO_2 input stream on the mole flow of CO_2.

Temperature	1 kmol/hr	26 kmol/hr	51 kmol/hr	76 kmol/hr	100 kmol/hr
10 C	0.804703	25.2996	49.7887	74.2995	97.8456
25 C	0.805893	25.3389	49.8731	74.4118	97.9708
40 C	0.807155	25.3709	49.9273	74.4746	98.0375
50 C	0.808004	25.3881	49.9512	74.4998	98.0638

Table 4.26: The effect of total mole flow and pressure of CO_2 input stream on the mole flow of CO_2.

Pressure	10 kmol/hr	35 kmol/hr	60 kmol/hr	85 kmol/hr	100 kmol/hr
15 bar	9.64968	34.2103	58.7621	83.3076	98.0343
20 bar	9.64925	34.209	58.7604	83.3059	98.0325
25 bar	9.64895	34.2081	58.7593	83.3047	98.0313

Table 4.27: The effect of total temperature and pressure of CO_2 input stream on the mole flow and mole fraction of CO_2.

X CO2	10 ^{0}C	40 ^{0}C	70 ^{0}C	100 ^{0}C	130 ^{0}C	160 ^{0}C	190 ^{0}C	200 ^{0}C
15 bar	0.985743	0.983492	0.978349	0.969837	0.957596	0.942243	0.92458	0.918305
20 bar	0.985754	0.983555	0.97835	0.969833	0.957597	0.942242	0.924579	0.918305
25 bar	0.985764	0.983597	0.97835	0.969833	0.957597	0.942242	0.924579	0.918305
30 bar	0.985773	0.98363	0.97845	0.969833	0.957597	0.942242	0.924579	0.918305
35 bar	0.985782	0.983656	0.978581	0.969833	0.957597	0.942242	0.924579	0.918305

N CO2	10 ^{0}C	60 ^{0}C	110 ^{0}C	160 ^{0}C	210 ^{0}C	250 ^{0}C
15 bar	97.8417	98.0806	98.1225	98.142	98.1564	98.166
40 bar	97.8281	98.0767	98.1224	98.1419	98.1564	98.166
65 bar	97.8103	98.0748	98.1224	98.1419	98.1564	98.166
90 bar	97.7735	98.0734	98.1224	98.1419	98.1564	98.166
100 bar	97.7413	98.0729	98.1224	98.1419	98.1564	98.166